→ 6th ESA ADVANCED TRAINING COURSE ON LAND REMOTE SENSING

Advanced SAR II: An introduction to interferometry

Ramon Hanssen

Delft University of Technology (TU Delft)
The Netherlands
e-mail: r.f.hanssen@tudelft.nl / Web: www.tudelft.nl/hanssen

Interferometry: mapping the millimeter

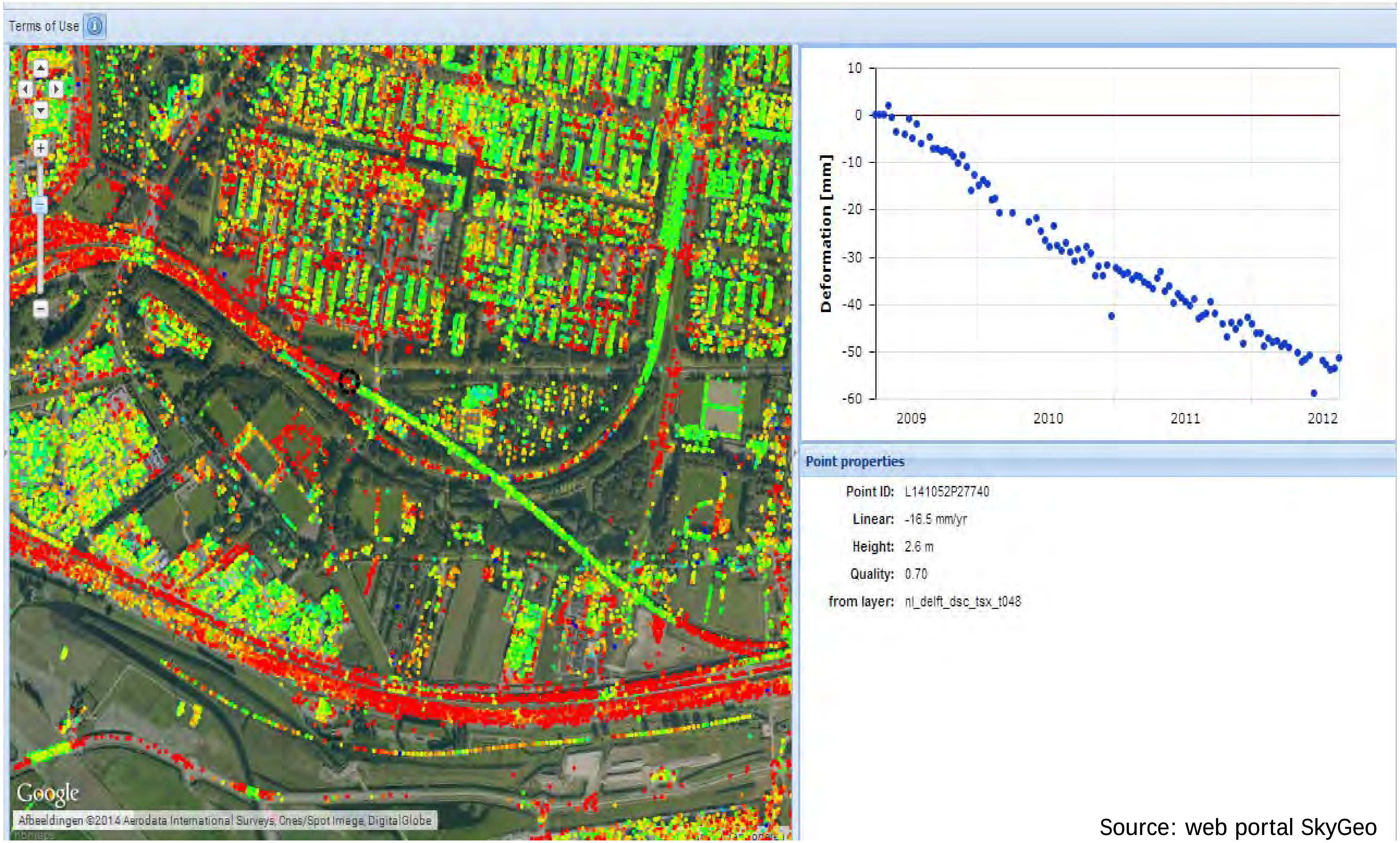

Source: web portal SkyGeo

Prior knowledge

- Radar principles, wavelength indications, SAR concept, resolution, satellite orbits, scattering,...
- Basic calculus: complex numbers, (rectangular form, polar form, exponential form), trigonometry,...

Learning objectives

- Interferometry: intuitive approach, physical approach
- Understanding sensitivity
- Basic observables and variables, concepts
- Practical data processing
- Quality control

A primer on satellite orbits

Kepler elements

I	inclination
Ω	longitude of the ascending node
e	eccentricity
ω	argument of perigee
a	semimajor axis
M	mean anomaly

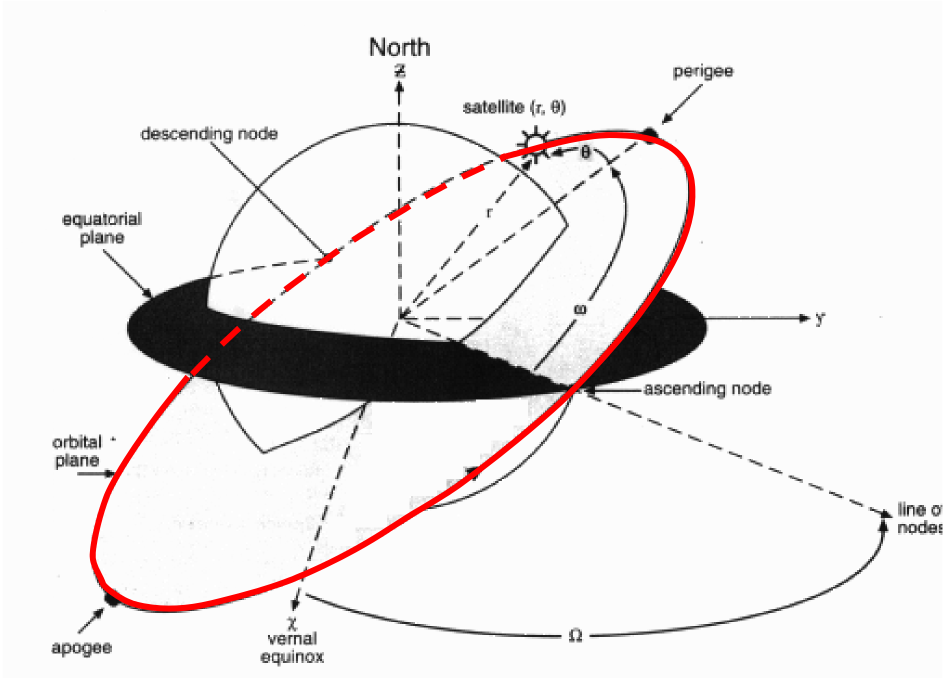

Great Keppler explanation YouTube
https://www.youtube.com/watch?v=cf9Jh44kL20

Satellite orbit

S	-	satellite
E	-	Earth
A	-	apogee
P	-	perigee
a	-	semimajor axis
b	-	semiminor axis
e	-	eccentricity

$$e^2 = \frac{a^2 - b^2}{a^2}$$

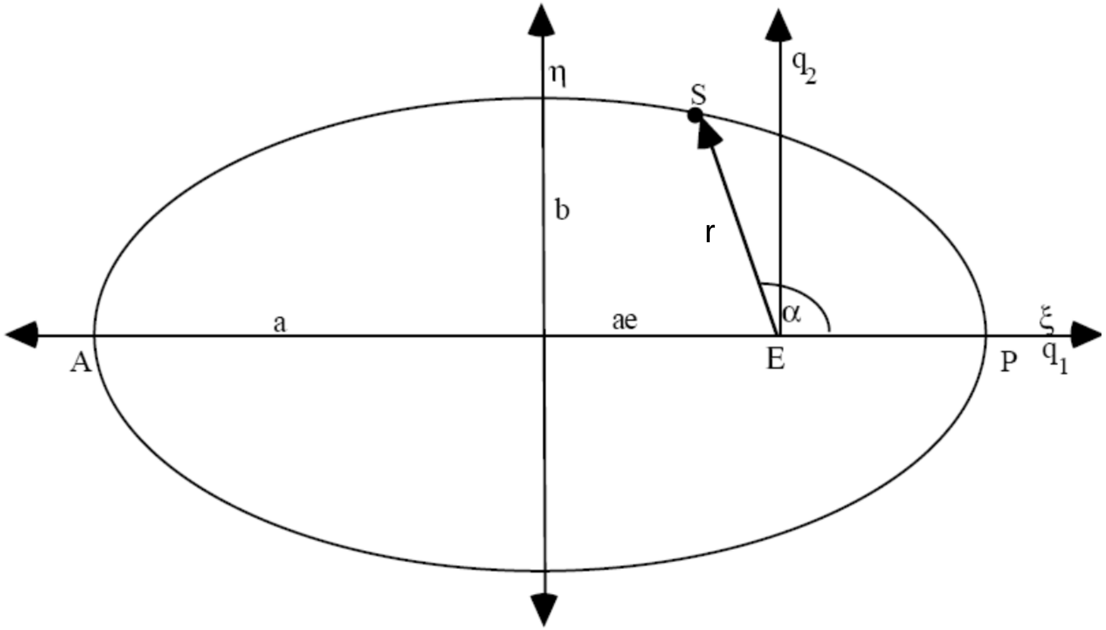

$$\frac{\xi^2}{a^2} + \frac{\eta^2}{b^2} = 1 \quad \Rightarrow \quad r = \frac{a(1-e^2)}{(1 + e\cos\alpha)}$$

$$\text{check} \Rightarrow \alpha = 0 \;\Rightarrow r = a\frac{(1+e)\,(1-e)}{(1+e)}$$

Orbit angular frequency: $\omega_o = \left(\frac{GM}{a^3}\right)^{1/2}$

Orbit period: or $P_o = \frac{2\pi}{\omega_o}$.

G = 6.67 x 10^{-11} N-m^2 /kg^2
$M_\oplus$ = 5.97 × 10^{24} kg
Gravitational constant: $GM_\oplus$ = 3.98 × 10^{14} N-m^2 /kg

Satellite orbits for EO purposes

Complications due to Earth flattening

Gravitational potential of the oblate Earth

$a_e \approx 6\,378\,135\text{m}$

$J_2 \approx 0.00108263$

$$V = -\frac{GM}{r}\left(1 - \frac{a_e^2 J_2}{2r^2}\,(3\sin^2 b - 1) + \ldots\right)$$

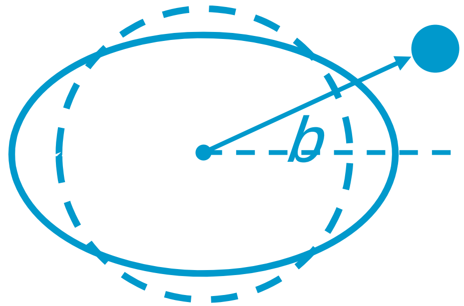

J_2 expresses the ‘oblateness’ of earth. It leads to to
1) increased orbital period 2) <u>precession</u> of orbital plane

Satellite orbits for EO purposes

Complications due to J2: Earth flattening

I	inclination
Ω	longitude of the ascending node
e	eccentricity
ω	argument of perigee
a	semimajor axis
M	mean anomaly

- Change of the longitude of the ascending node

$$\frac{d\Omega}{dt} = s\ \cos I \qquad s = c_{2,0}\frac{3}{2}\sqrt{\frac{GM}{a^3}}\left(\frac{a_e}{a(1-e^2)}\right)^2$$

- Change of the argument of the perigee

$$\frac{d\omega}{dt} = \frac{s}{2}\left(1 - 5\cos^2 I\right)$$

$$GM = 3.98600434 \cdot 10^{14}[\mathrm{m}^3/\mathrm{s}^2]$$

- Change of the mean motion

$$a_e \approx 6\ 378\ 135\mathrm{m}$$

$$\frac{dM}{dt} = -\frac{s}{2}\sqrt{1-e^2}\left(3\cos^2 I - 1\right)$$

$$J_2 = -c_{2,0} = 0.00108263$$

Satellite orbits for EO purposes

Complications due to Earth flattening

Keplerian orbital period

inclination

Increased orbital period

$$P_n = 2\pi\sqrt{\frac{a^3}{GM}}\left(1+\frac{3J_2 a_e^2}{4a^2}\left\{1-3\cos^2 i+\frac{1-5\cos^2 i}{(1-e^2)^2}\right\}\right)$$

semi-major axis

eccentricity

$$\Omega_p = -\frac{3\, J_2\, \sqrt{GM}\; a_e^2\; a^{-7/2}\;\; \cos i}{2(1-e^2)^2}$$

Precession rate of orbital plane

Satellite orbits for EO purposes

Complications due to Earth flattening

- → Change of the orbital period (time for one revolution)

  - From
  $$P_0 = \frac{2\pi}{n}, \quad n = \sqrt{\frac{GM}{a^3}}$$
  - to
  $$P_n = \frac{2\pi}{n + \dot{\omega} + \dot{M}}$$

TU Delft

Satellite orbits for EO purposes

A number of special orbits are useful for EO, some utilizing the J2 effect

- Polar orbits (EO)
- Frozen orbits (EO)
- Sun-synchronous orbits (EO)
- Repeat orbits (EO)
- Geostationary orbits (telecommunication, meteo, relay)
- Molniya orbits (telecommunication)

Satellite orbits for EO purposes

Polar orbits

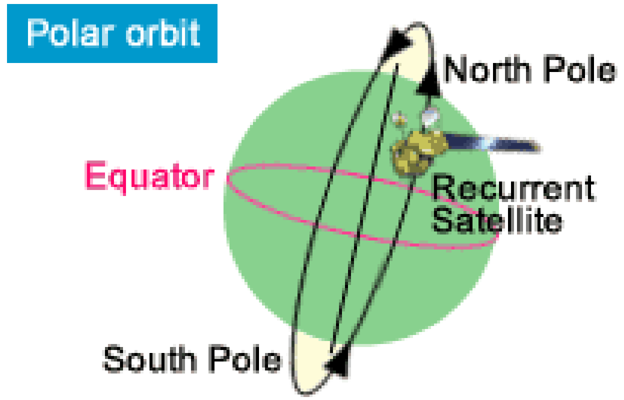

- Satellite passes the poles
  - → Inclination I=90 deg
  - → $d\Omega/dt = 0$, i.e. orbital plane does not change w.r.t. inertial space
  - Groundtracks cover Earth homogeneously

Satellite orbits for EO purposes

Sun-synchronous orbits

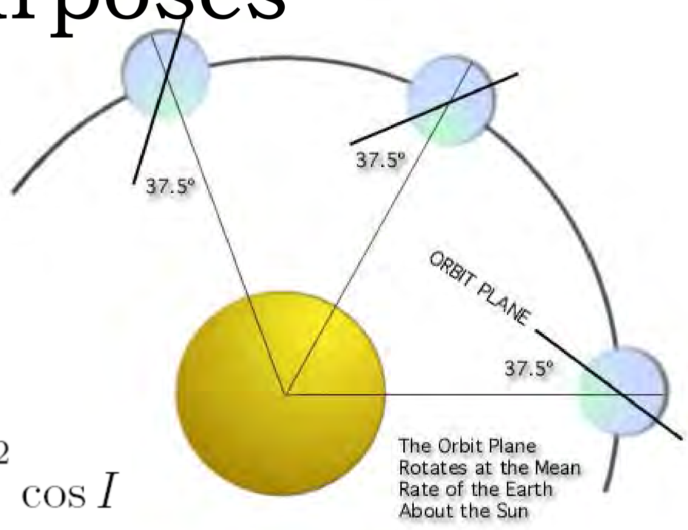

Precession rate of orbital plane

$$\frac{d\Omega}{dt} = \frac{2\pi}{365.25 \cdot 86400} \quad \text{[rad/s]}$$

$$\frac{d\Omega}{dt} = -2.01279544 \cdot 10^{-6}[rad/s]\frac{1}{(1-e^2)^2}\left(\frac{a_e}{a}\right)^{7/2}\cos I$$

Rees, Fig 10.14

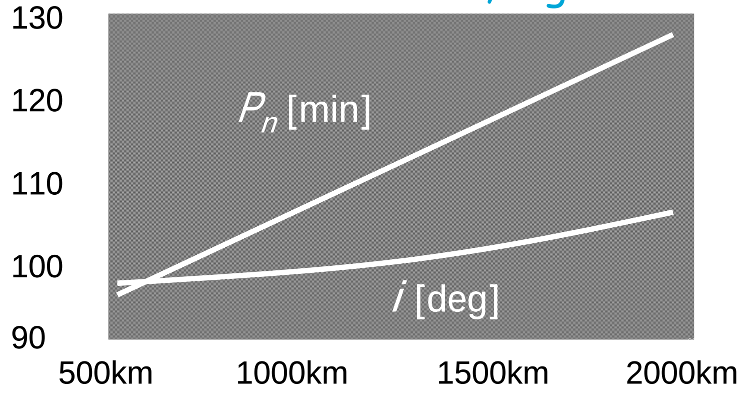

- Example: Sentinel-1
  - → $e \sim 0$, $a = a_e + 693$ km → $I = 98.18$ deg

Satellite orbits for EO purposes

Repeat orbits

Sub-satellite track forms a closed curve on the surface, so that a given position can be observed periodically

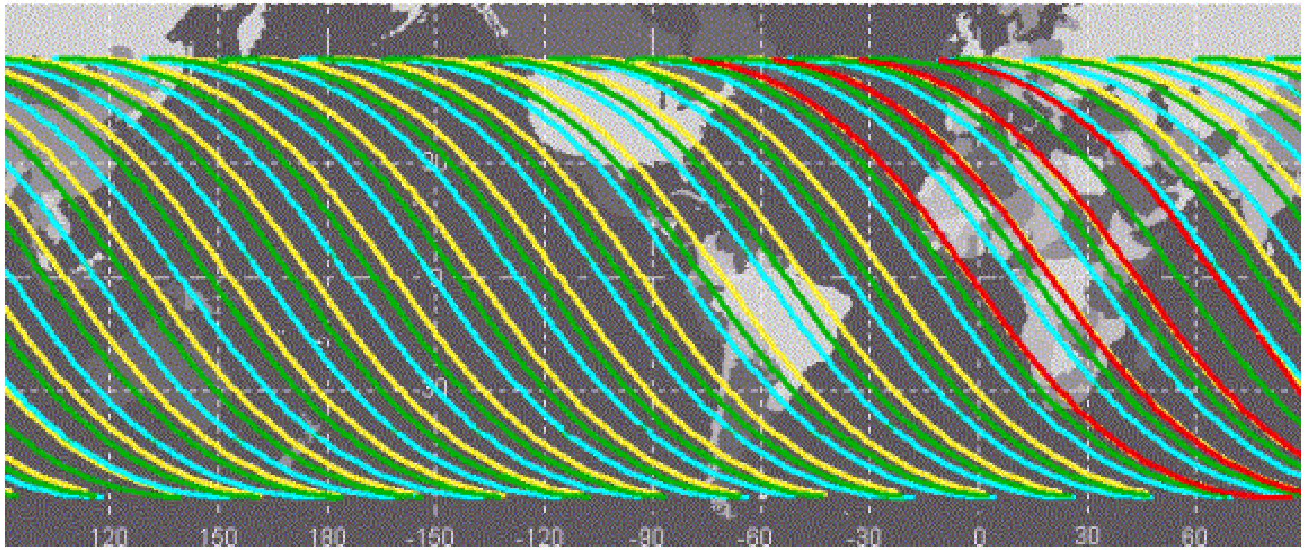

Repeat of orbits every 3 days for ISS. Orbits for Day 1 in yellow, day 2 in green, and day 3 in aqua. First four repeating orbits of the 4th day in red. ©NASA-Johnson Space Center

Satellite orbits for EO purposes

Repeat orbits

nd : repeat orbit [days]

nr : repeat orbit [revolutions]

- Without flattening

$$\frac{n_d}{n_r} \cdot n = \Omega_E \qquad \Omega_E = \frac{2\pi}{86400} \text{ [rad/s]}$$

- With flattening

$$\frac{n_d}{n_r} \cdot \left(n + \dot{\omega} + \dot{M} \right) = \Omega_E - \dot{\Omega}$$

Examples

- Sentinel-1 : $n_d = 12$, $n_r = 175$
- Topex/Poseidon: $n_d = 10$, $n_r = 127$
- LANDSAT: $n_d = 16$, $n_r = 233$
- ICESat: $n_d = 91$, $n_r = 1354$

Interferometry

14 May 2014: Oldest telescope of the Netherlands found at tunnel zone Delft (older than 1650)

Hans Lippershey’s patent, 1608

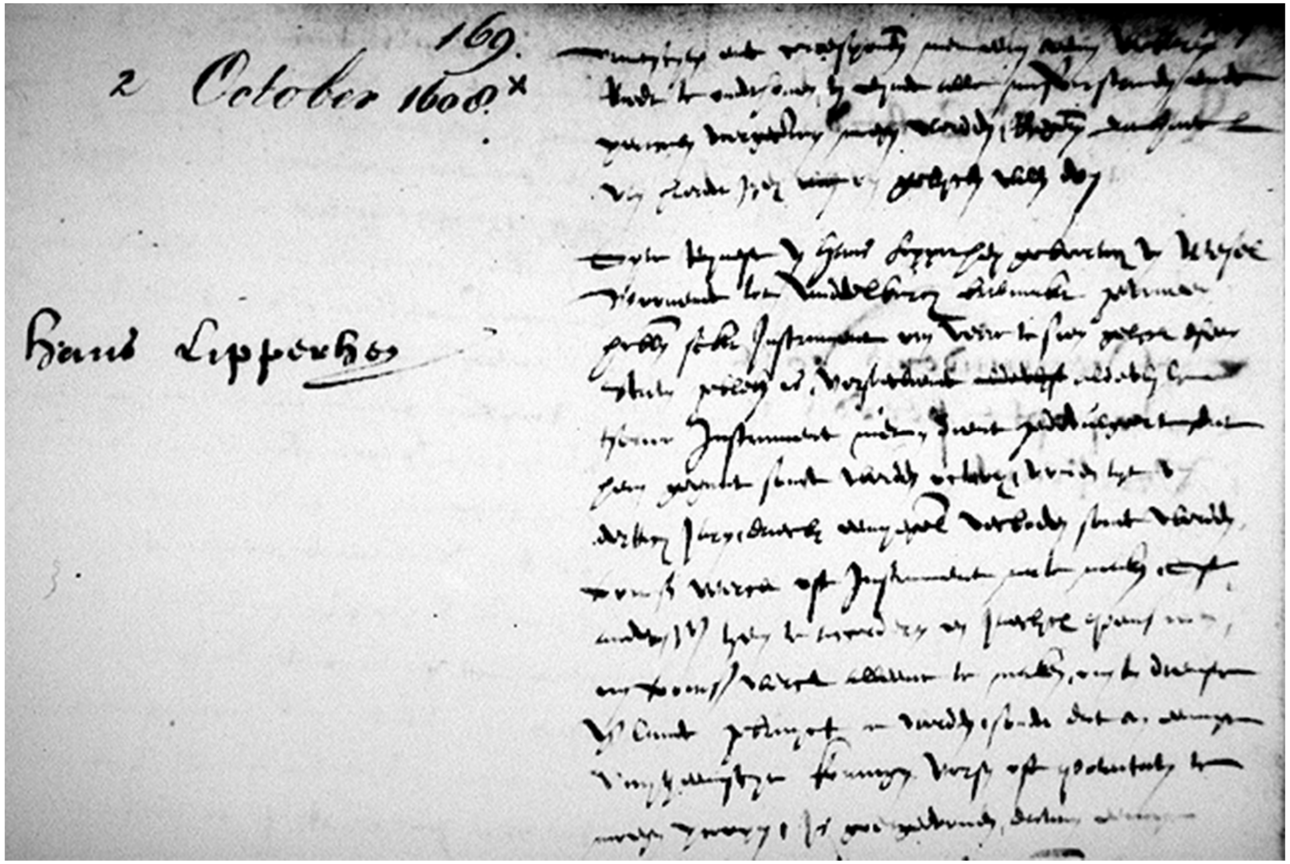

Christiaan Huygens (1678)

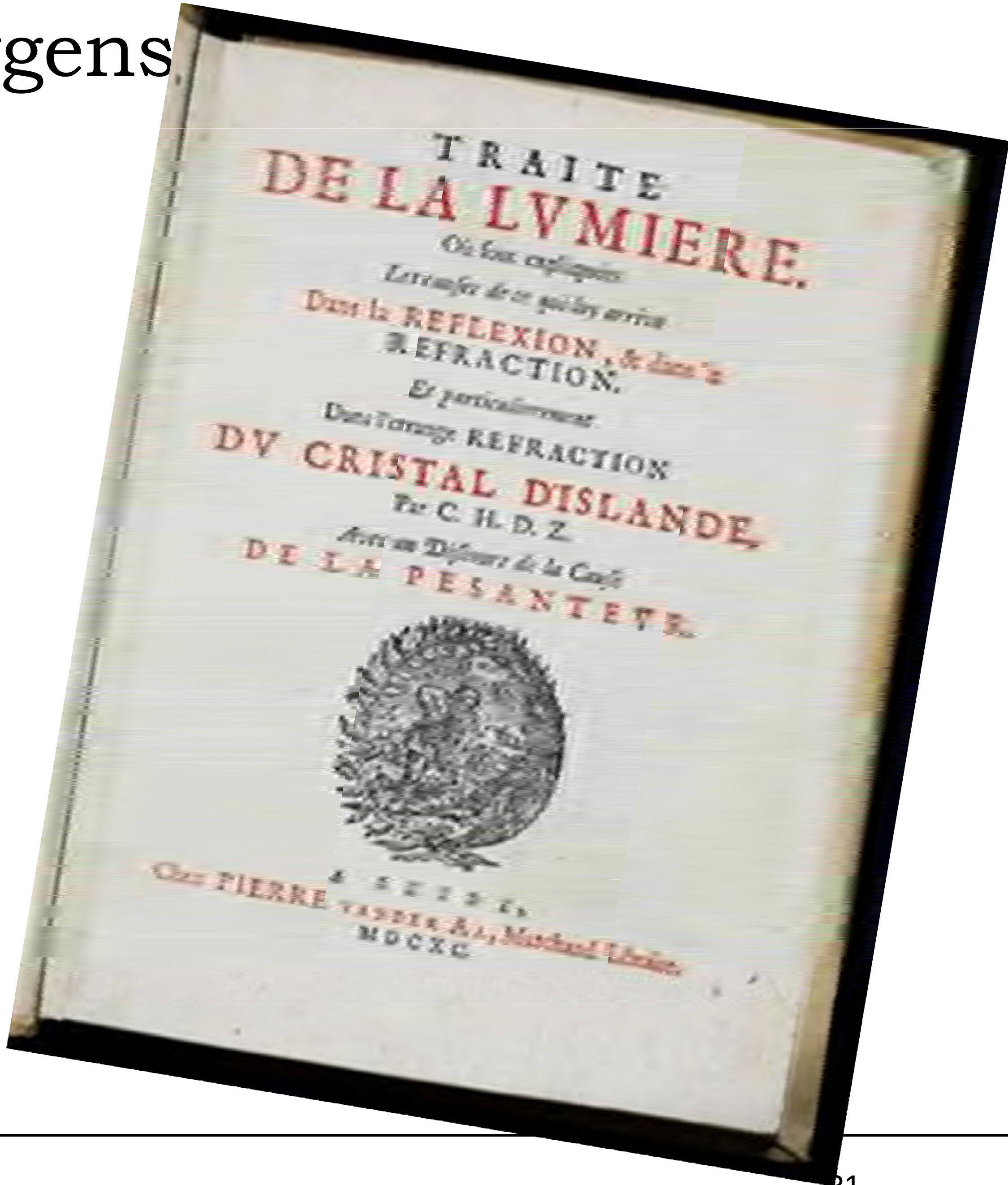

Mais il faut conſiderer encore plus particulierement l'origine de ces ondes, & la maniere dont elles s'eſtendent. Et premierement il s'enſuit de ce qui à eſté dit dela production de la lumiere, que chaque petit endroit d'un corps lumineux, comme le Soleil, une chandelle, ou un charbon ardent, engendre ſes ondes, dont cet endroit eſt le centre. Ainſi dans la flame d'une chandelle, eſtans diſtinguez les points A, B, C; les cercles concentriques, decrits autour de chacun de ces points, repreſentent les ondes qui en provienent. Et il en faut concevoir de meſme autour de chaque point de la ſurface, & d'une partie du dedans de cette flame.

1993

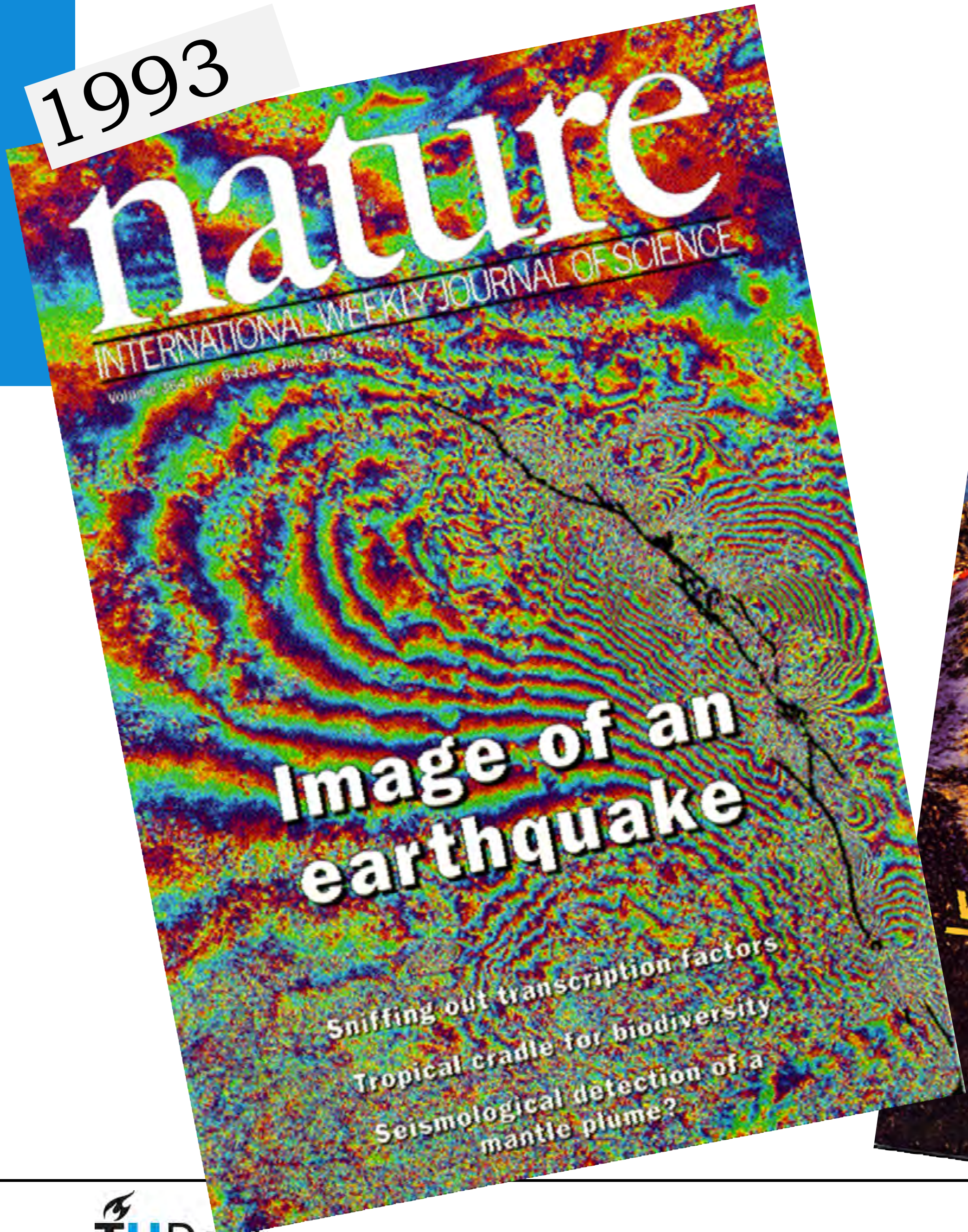
nature
INTERNATIONAL WEEKLY JOURNAL OF SCIENCE
Image of an earthquake
Sniffing out transcription factors
Tropical cradle for biodiversity
Seismological detection of a mantle plume?

1995

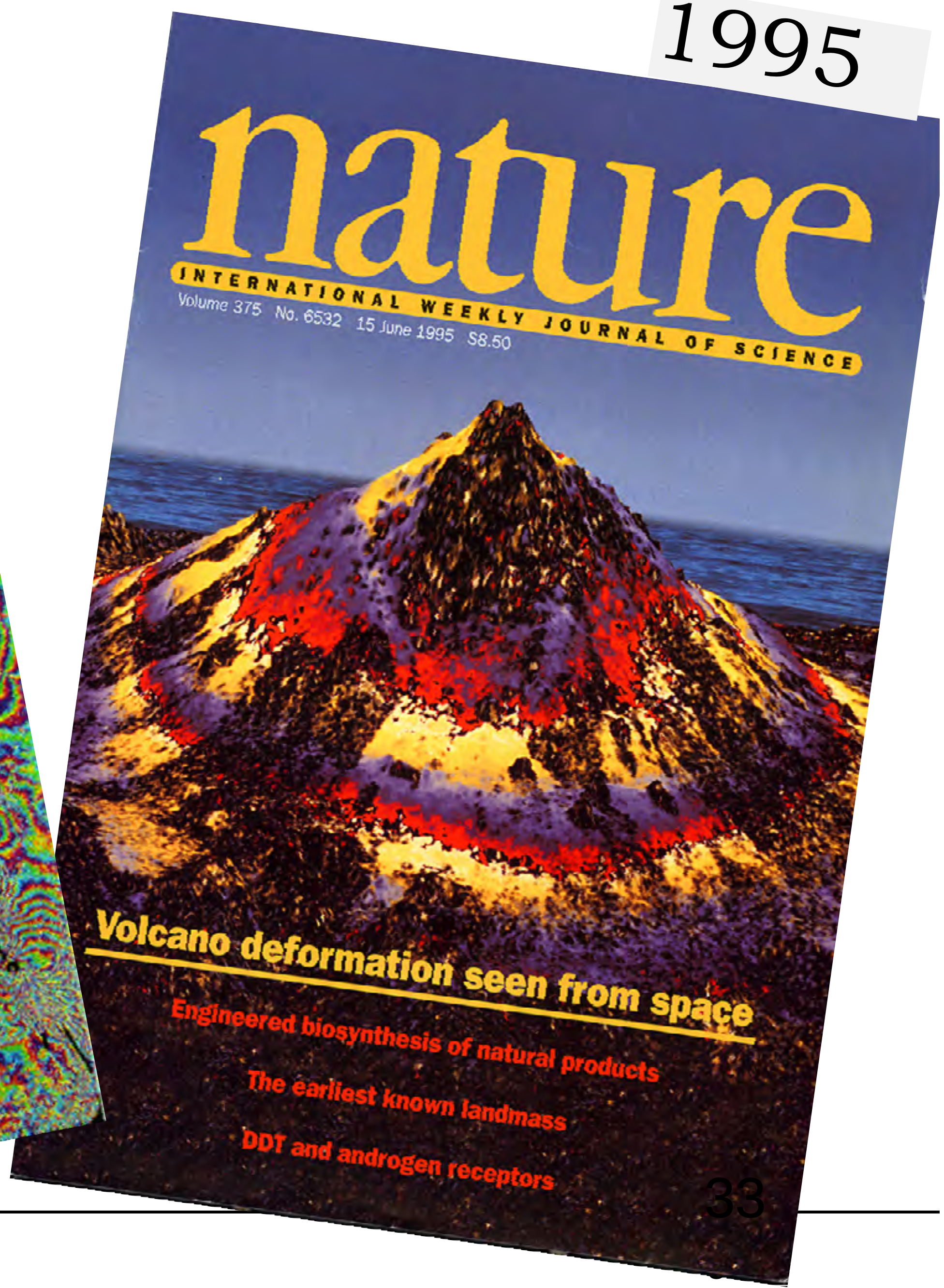
nature
INTERNATIONAL WEEKLY JOURNAL OF SCIENCE
Volume 375 No. 6532 15 June 1995 $8.50
Volcano deformation seen from space
Engineered biosynthesis of natural products
The earliest known landmass
DDT and androgen receptors

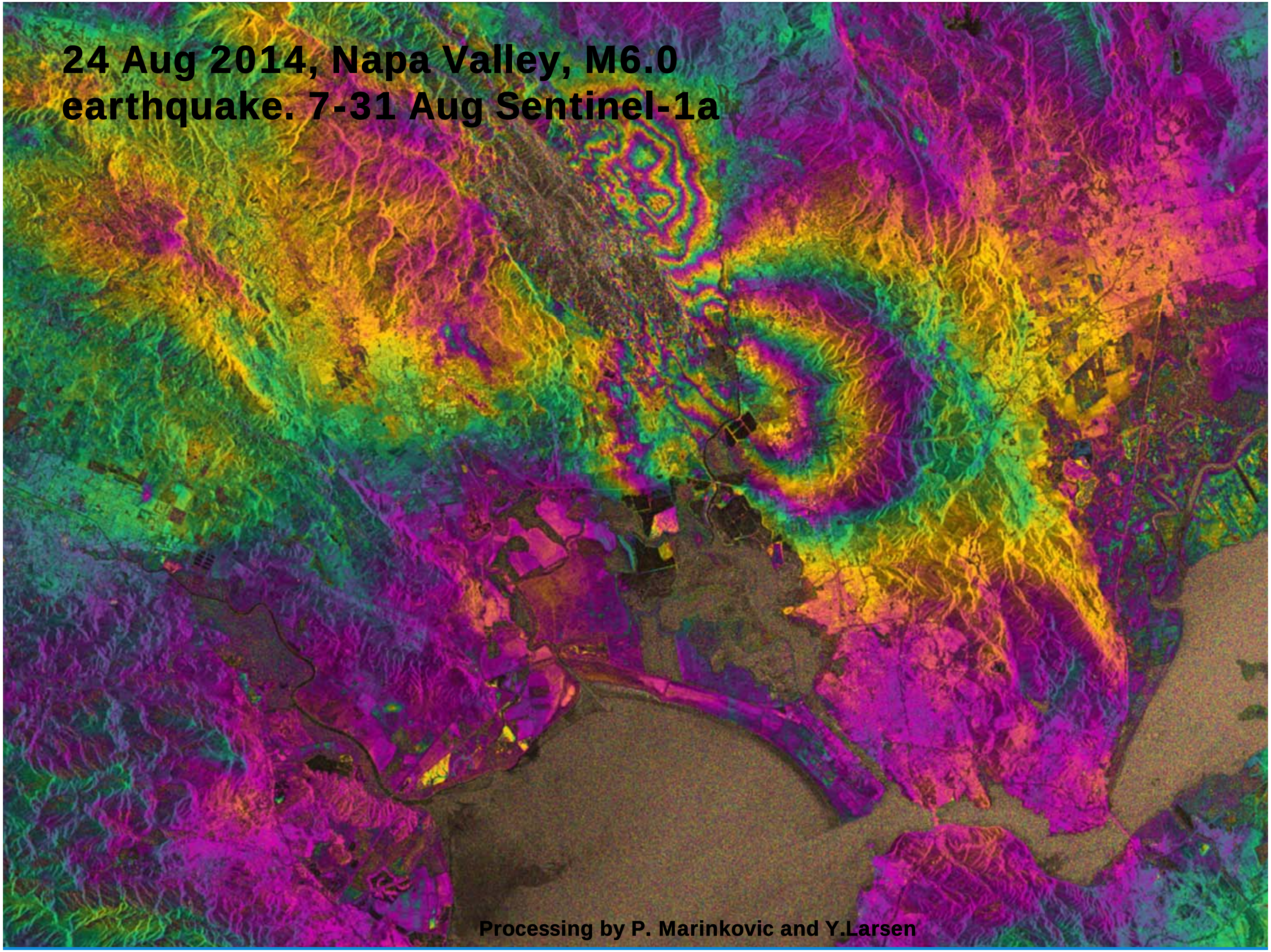
24 Aug 2014, Napa Valley, M6.0
earthquake. 7-31 Aug Sentinel-1a
Processing by P. Marinkovic and Y.Larsen

SAR SLC observations

SLC: Single-Look Complex data

- Single-look: no averaging, finest spatial resolution
- Complex: both real and imaginary (In-phase and quadrature phase) stored

Coherent imaging

$$y_1 = |y_1| \exp(j\psi_1)$$

Amplitude

Phase

Uninterpretable, due to scattering mechanism

Intuitive approach: geometry

Radar Interferometry

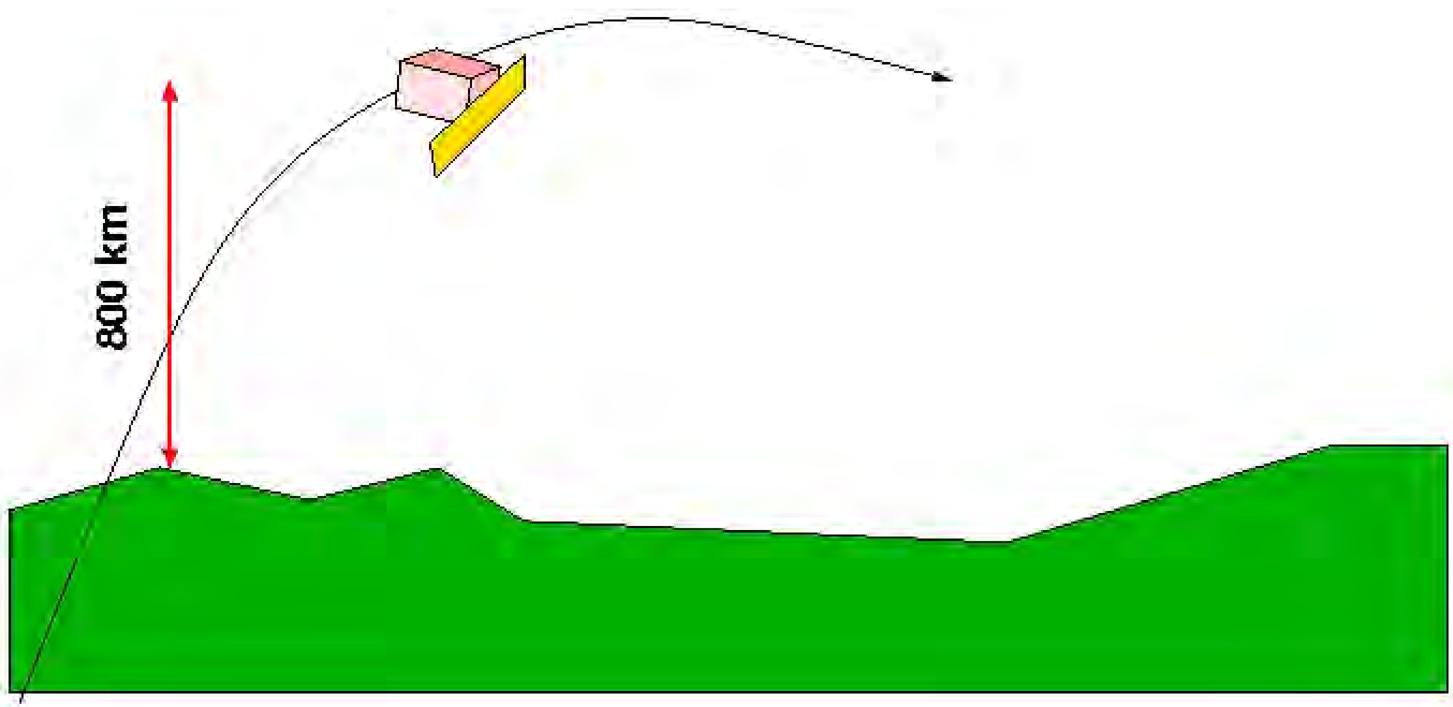

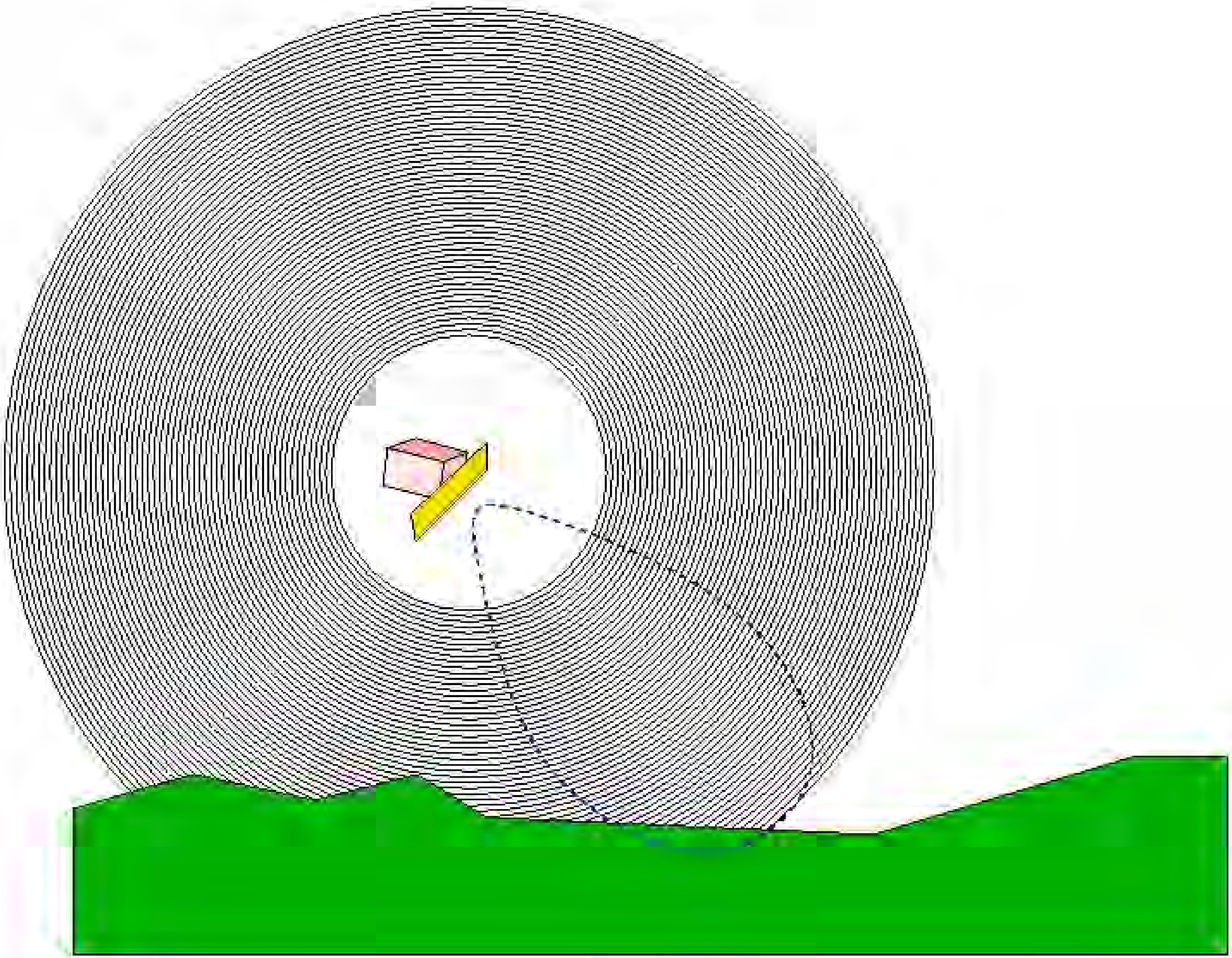

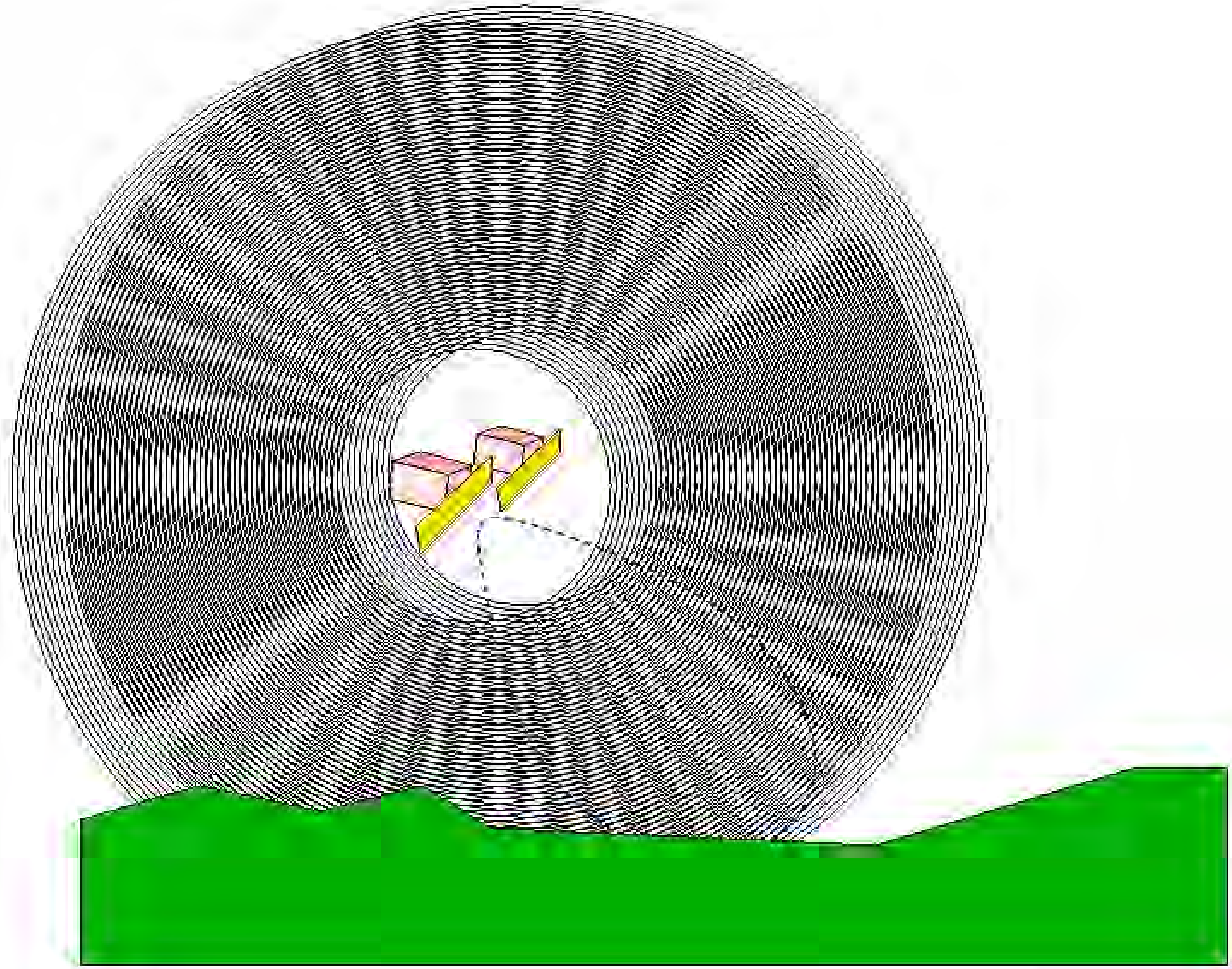

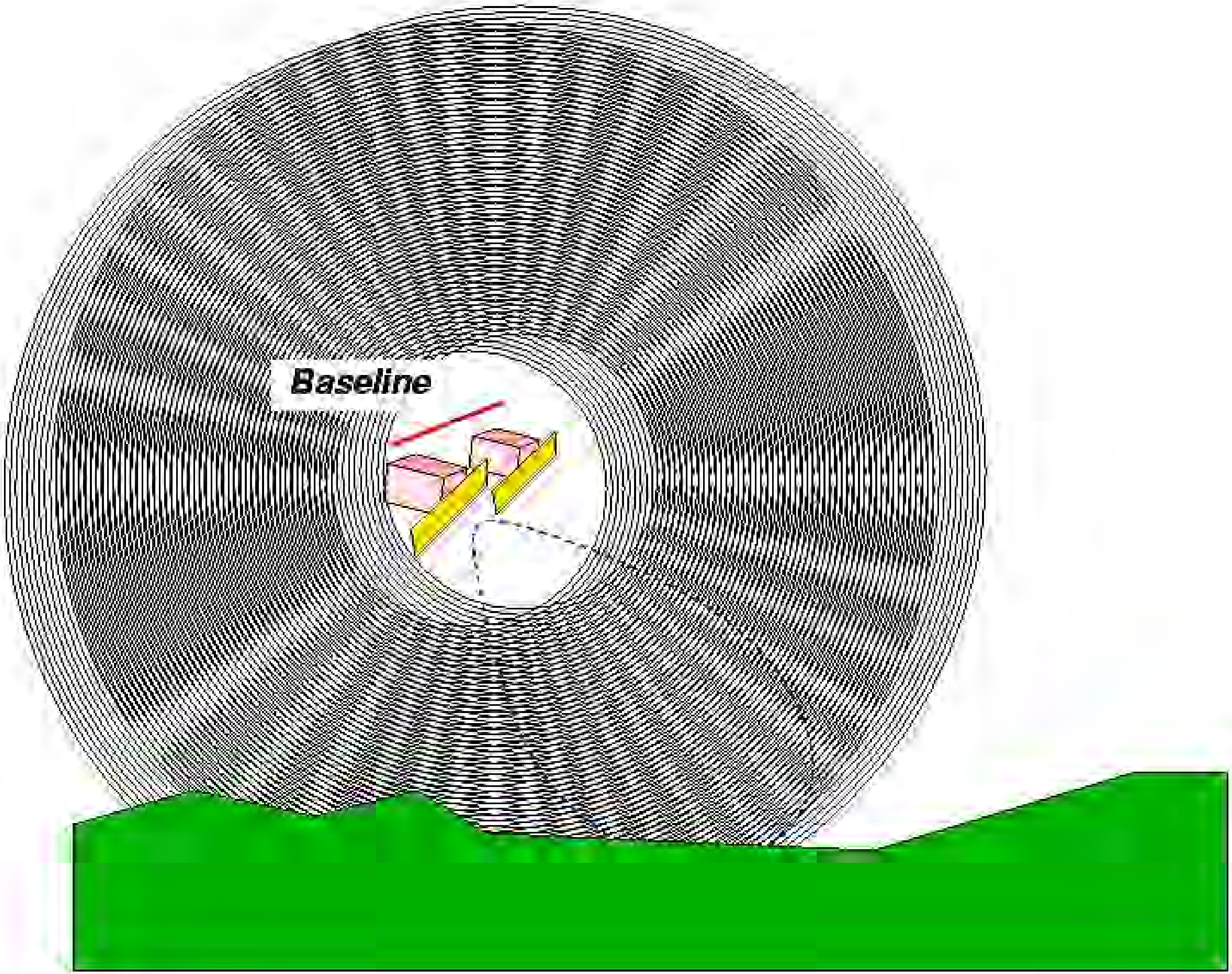
Baseline

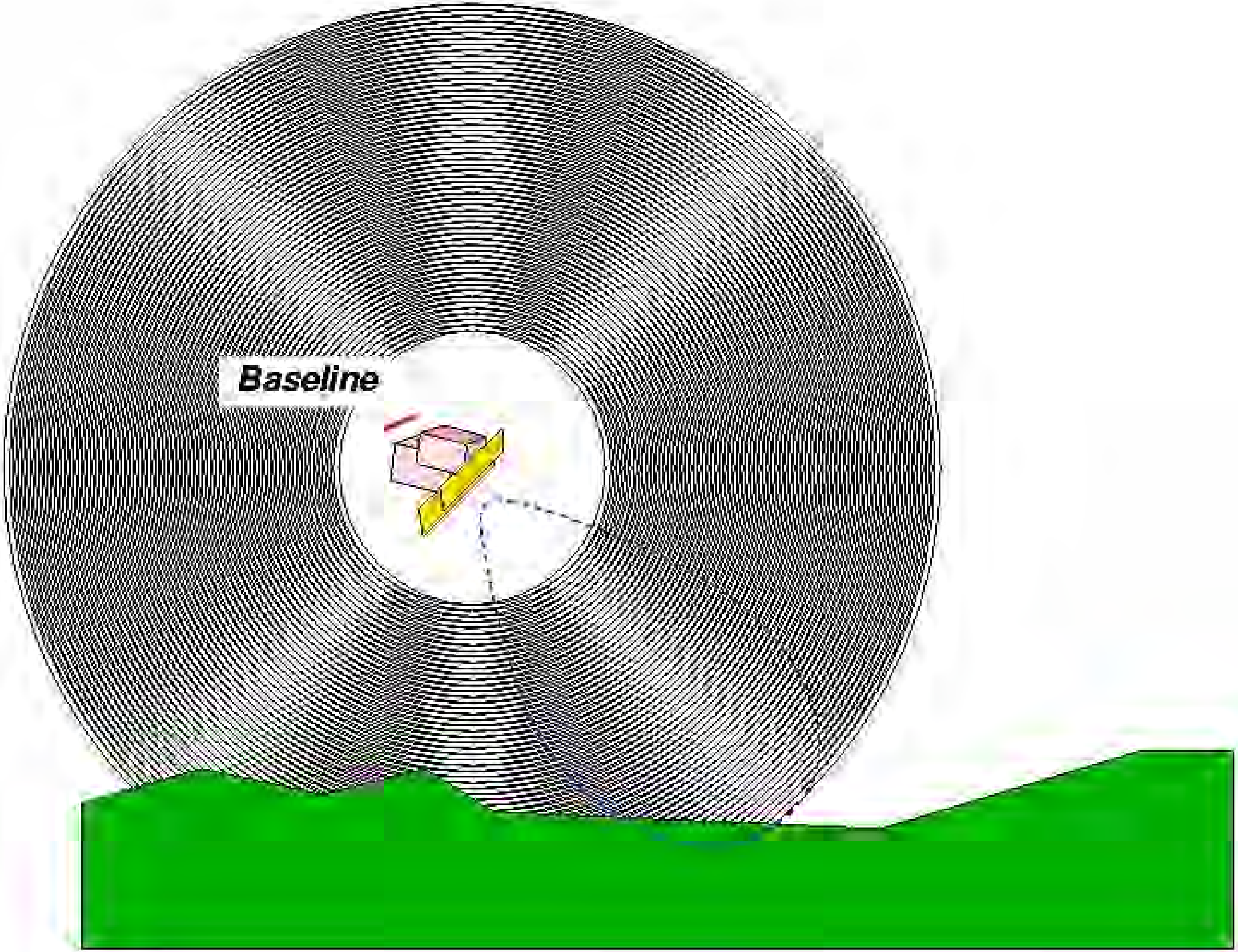
Baseline

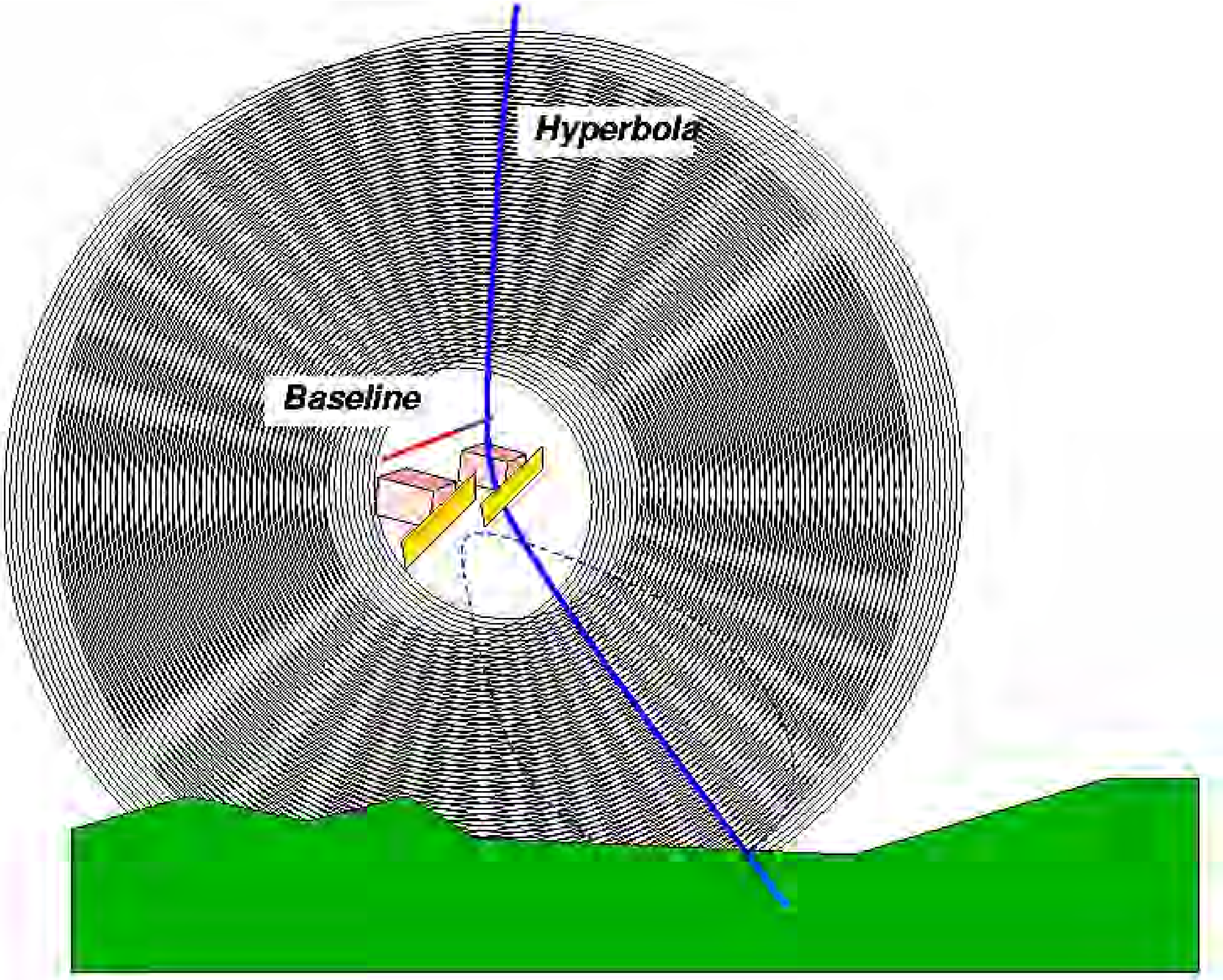
Hyperbola
Baseline

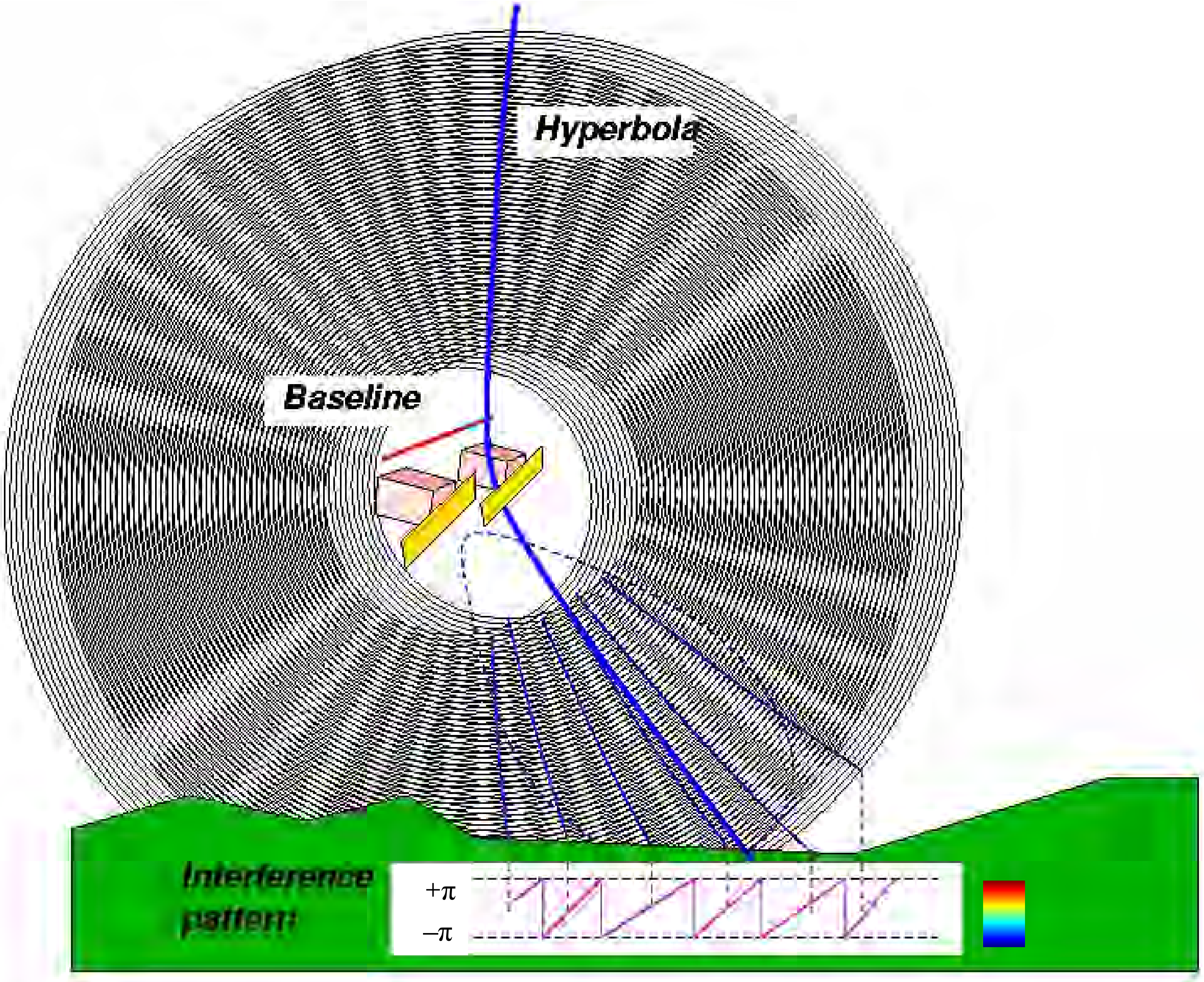
Hyperbola
Baseline
Interference pattern
+π
−π

Example in 2D: interferogram

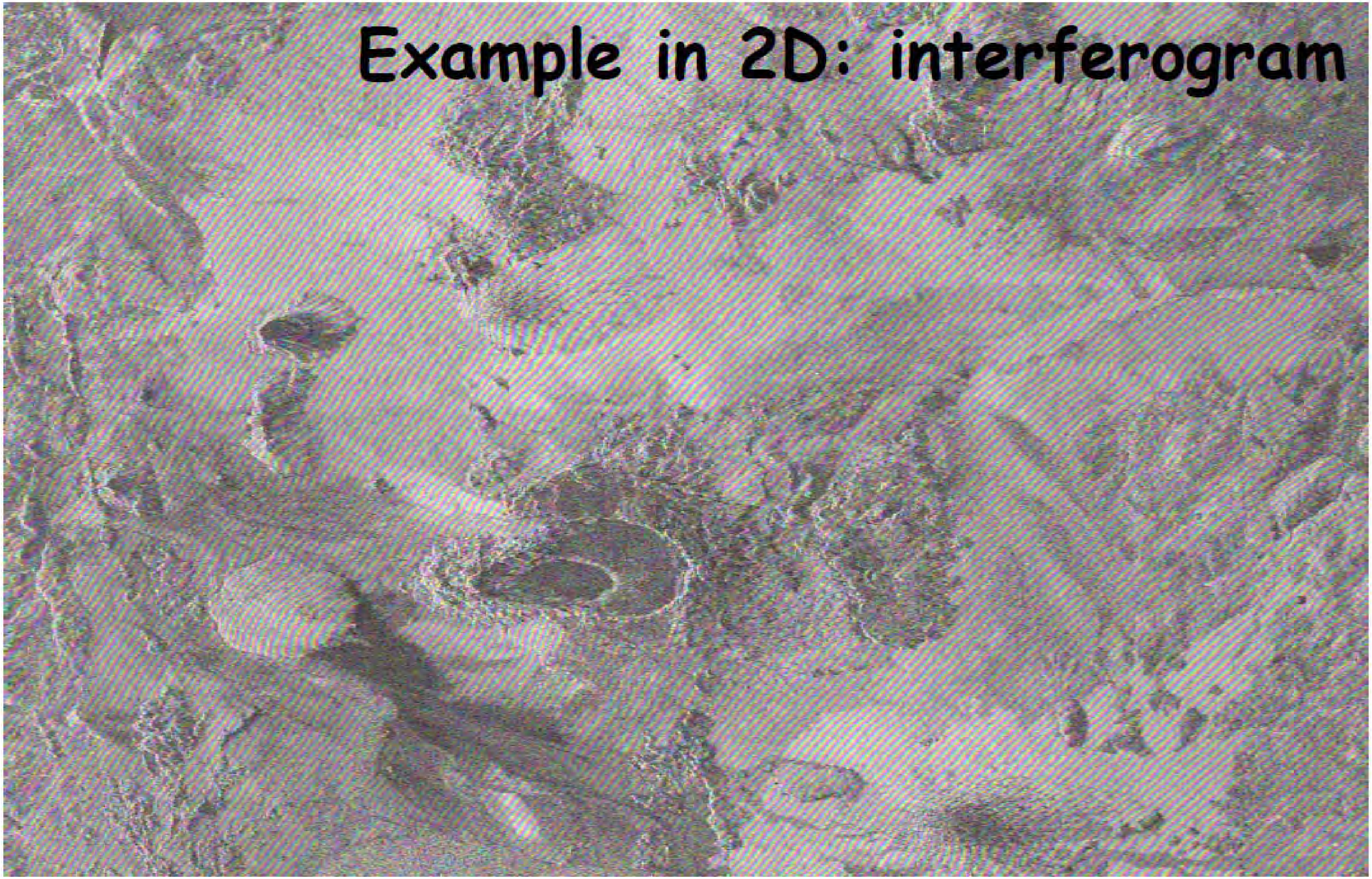

Range

Expressed as phase (radians)

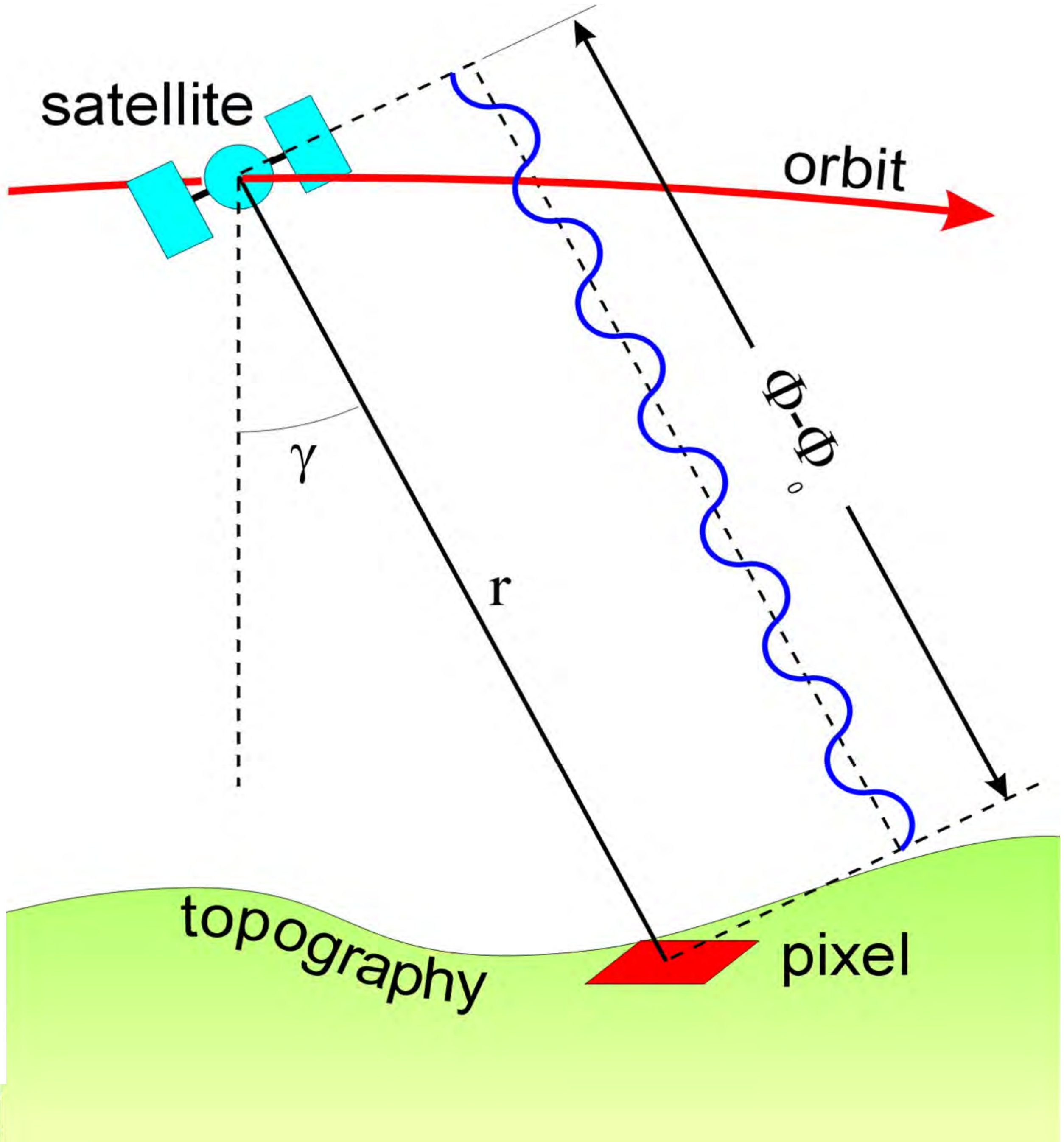

Range

Expressed as integer cycles + fractional phase

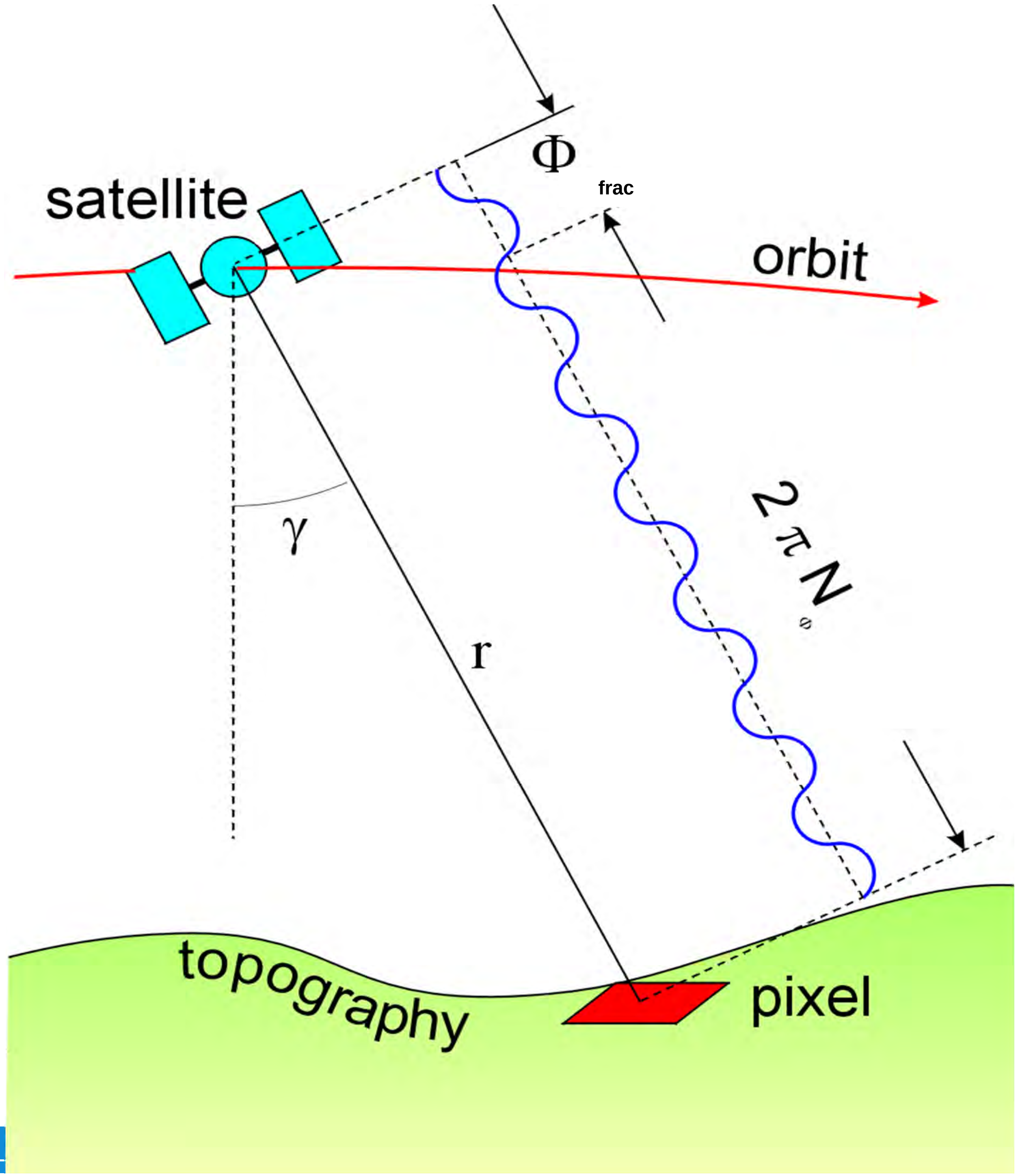

Two satellites: the 'baseline'

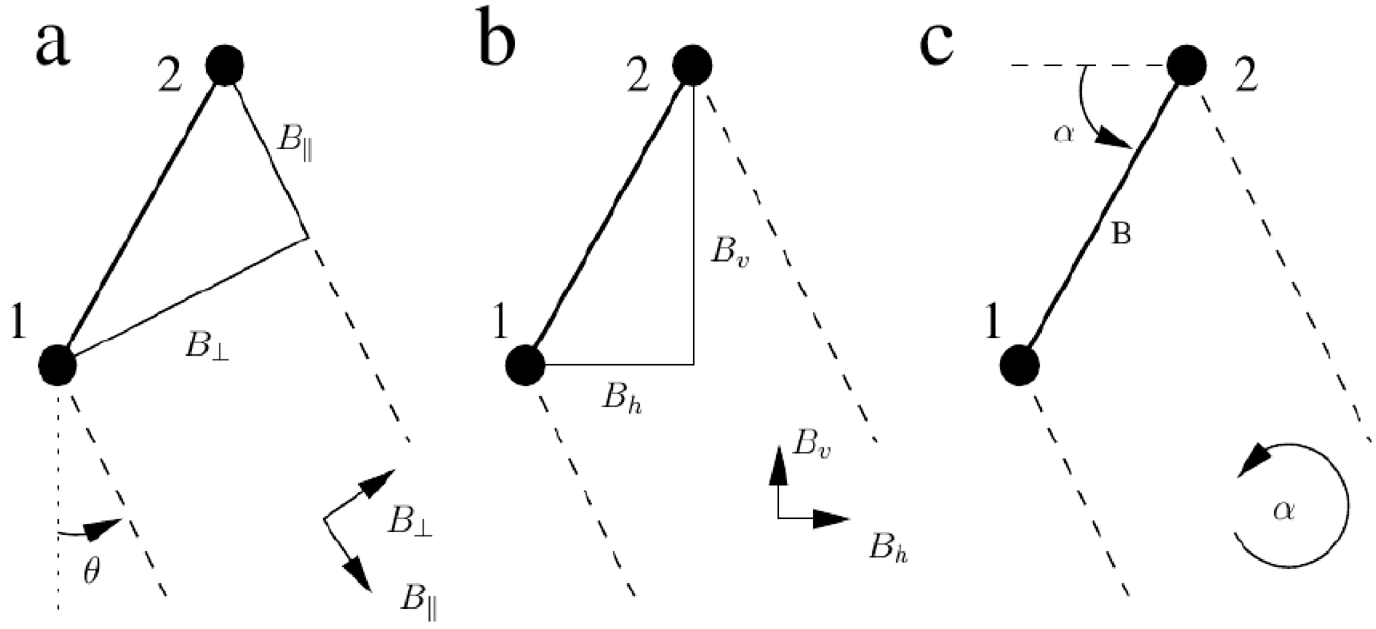

Figure B.2 Definition of the baseline parameters. (a) parallel/perpendicular; (b) horizontal/vertical; (c) length/orientation; Position 1 is the reference position. $B_{\|} > 0$ when $R_1 > R_2$, where R_i is the corresponding slant range. The angle α is defined counter-clockwise from the reference satellite (1), starting from the horizontal at the side of the look direction.

Reference phase (flat earth phase)

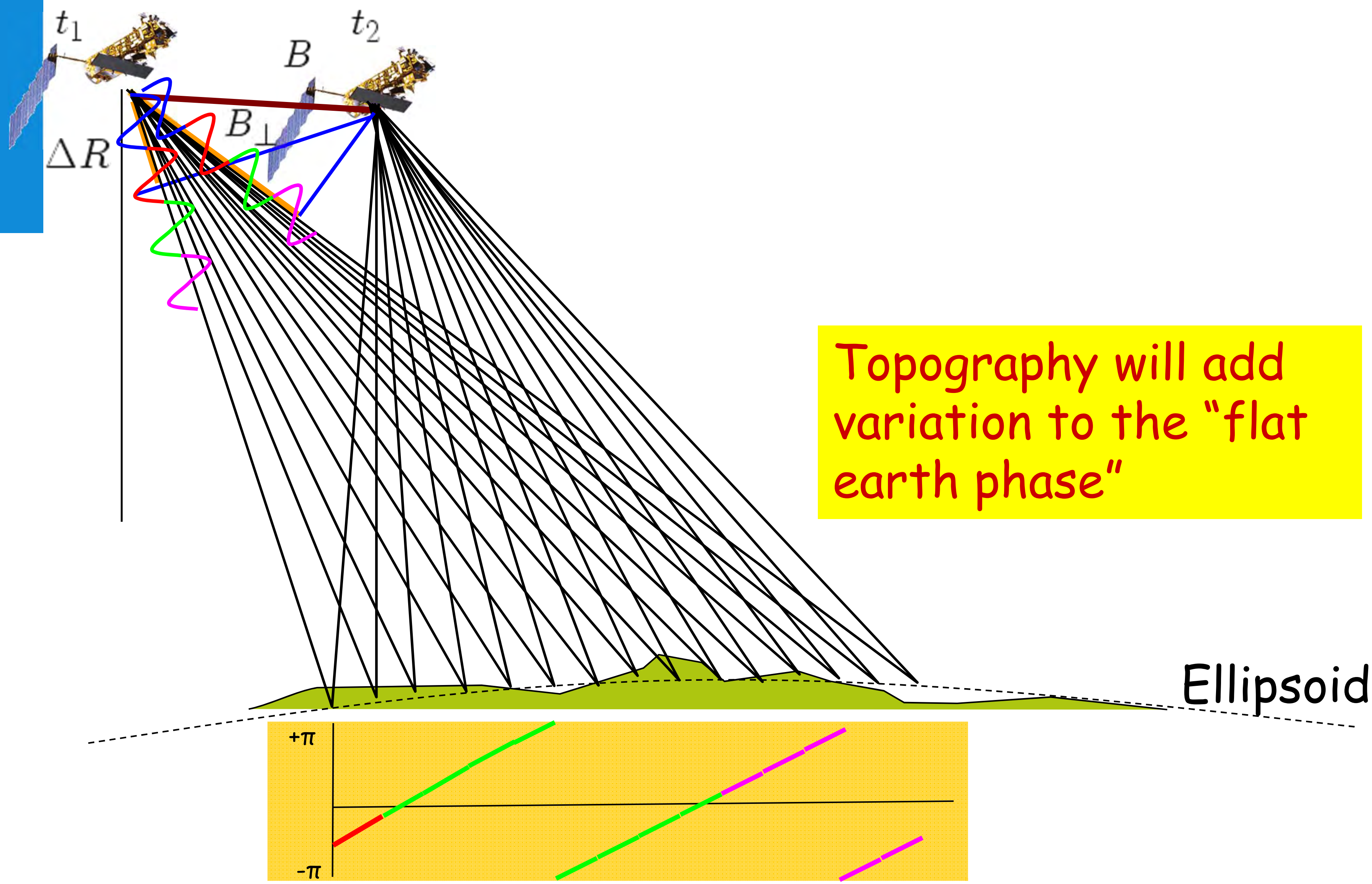

Topography will add variation to the "flat earth phase"

Example Reference Phase

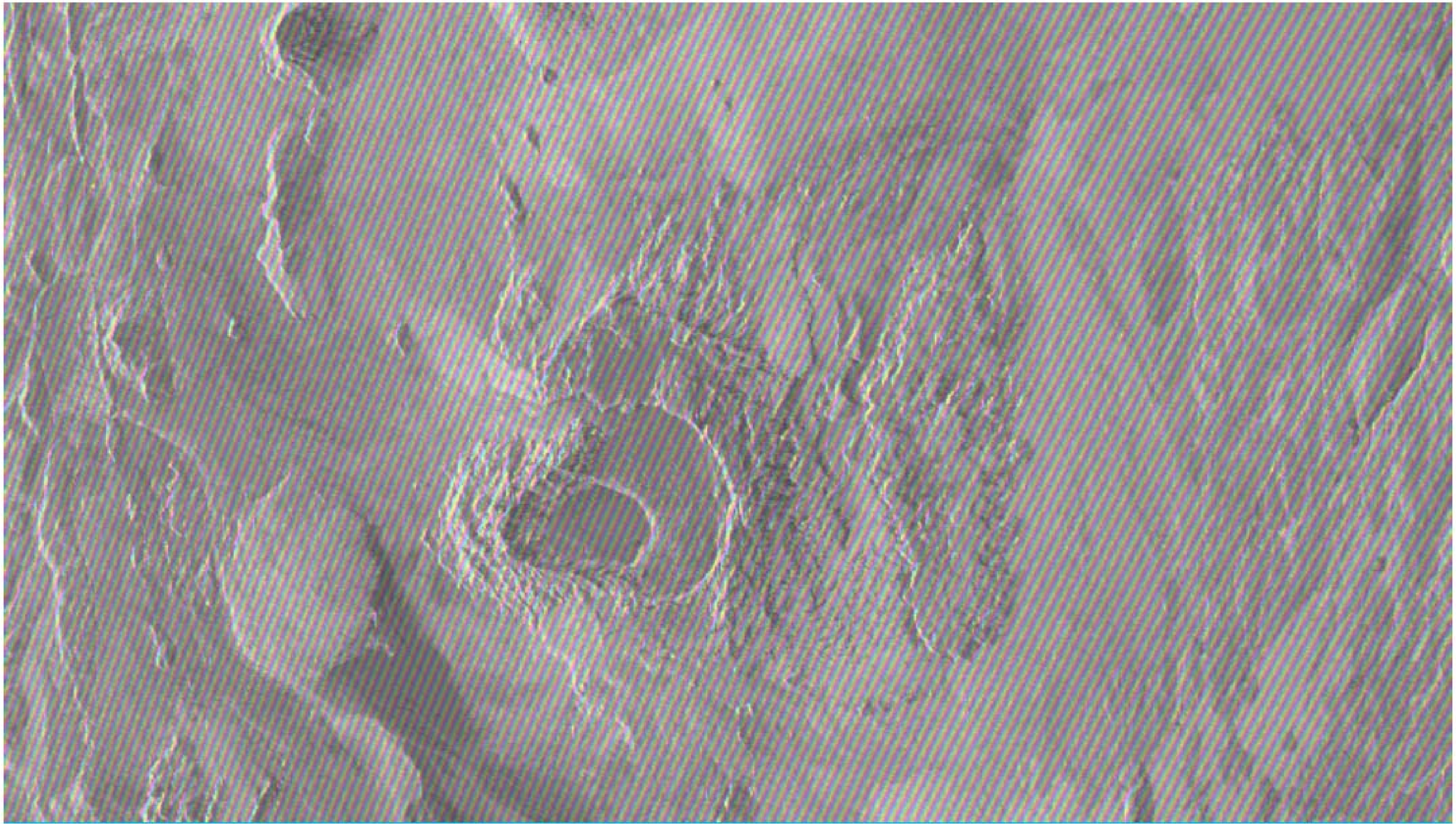

Topographic Phase

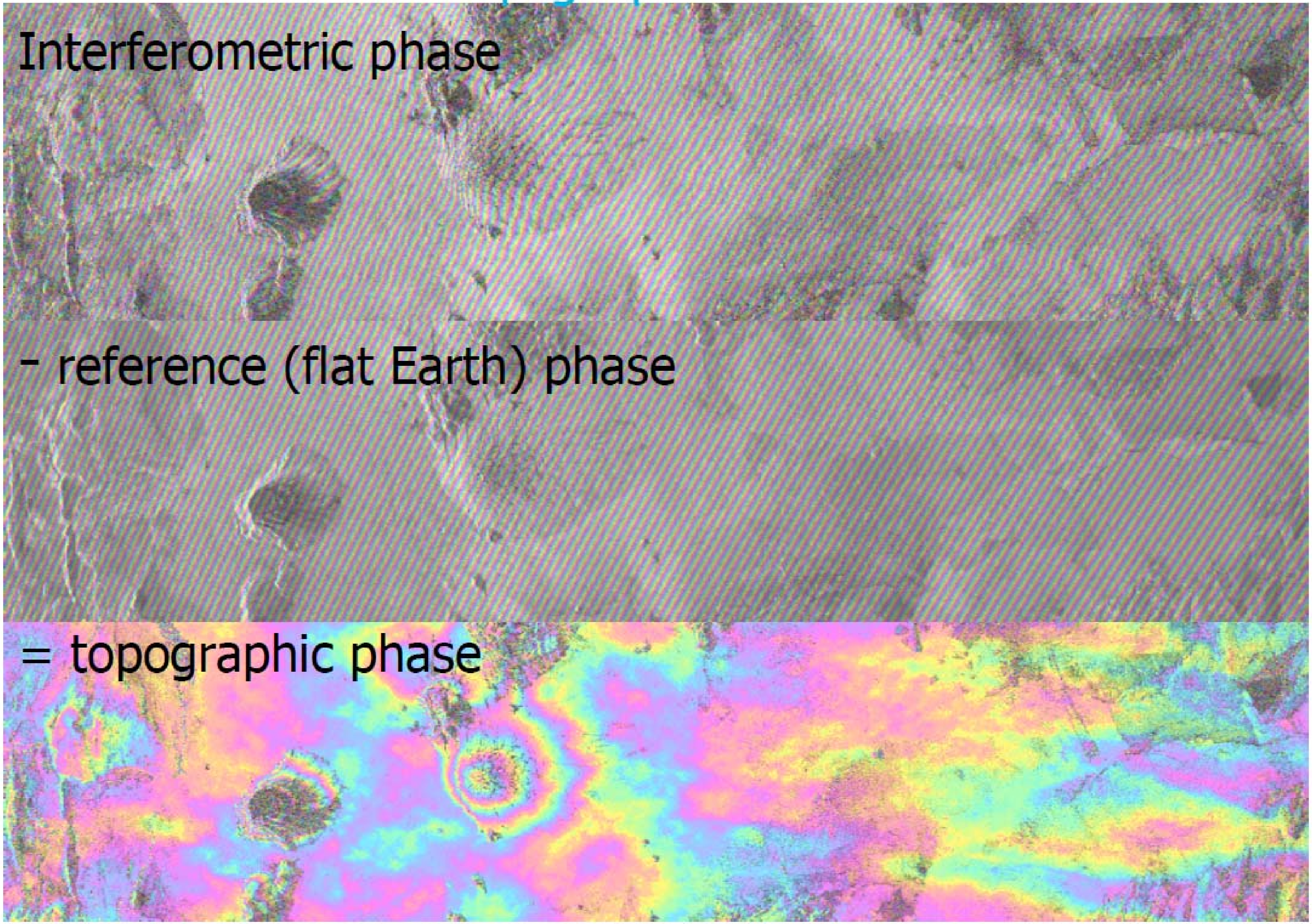

Example in 2D: interferogram

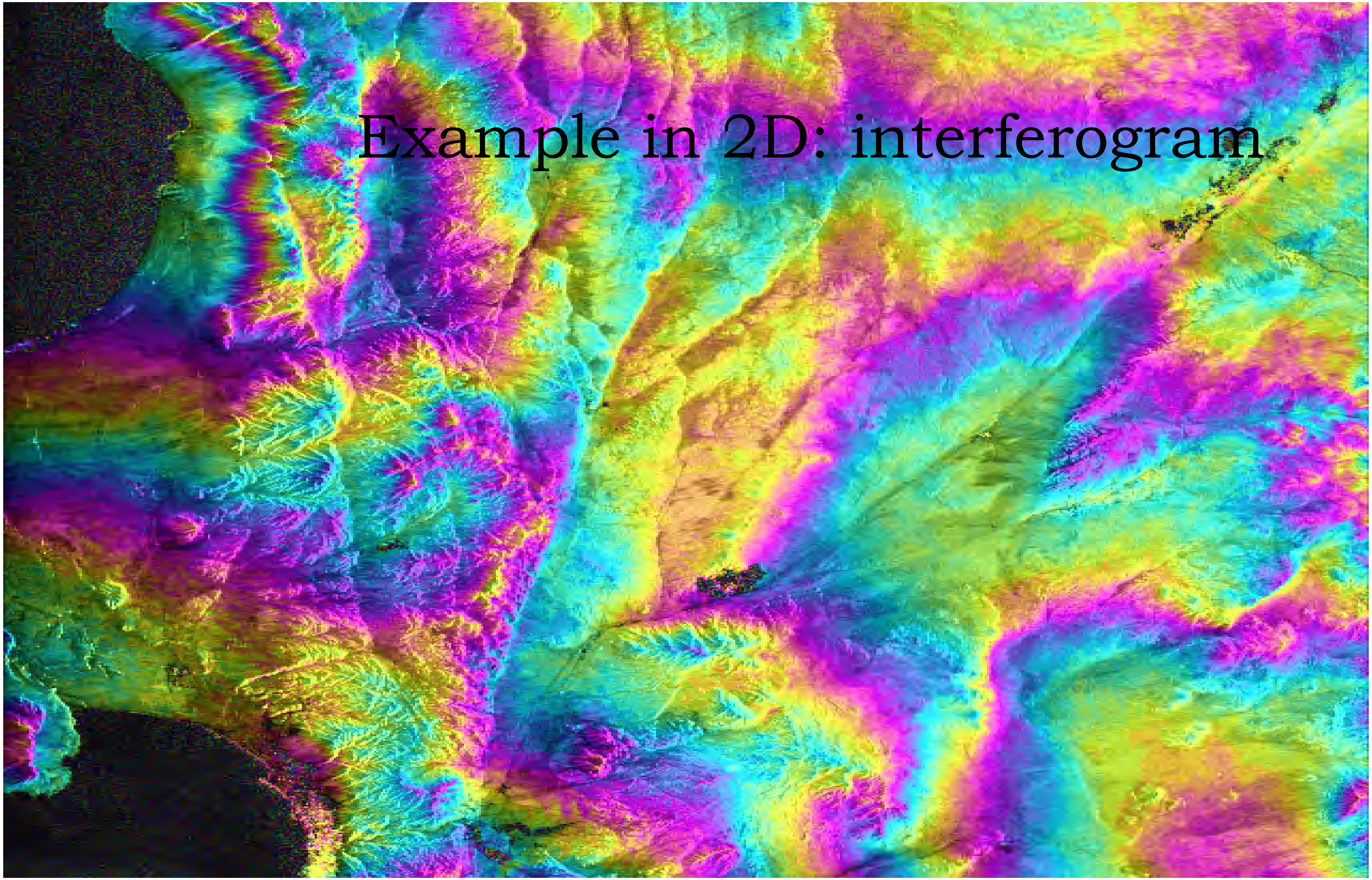

Interferometry:
deriving the equations

Phase-range relationship

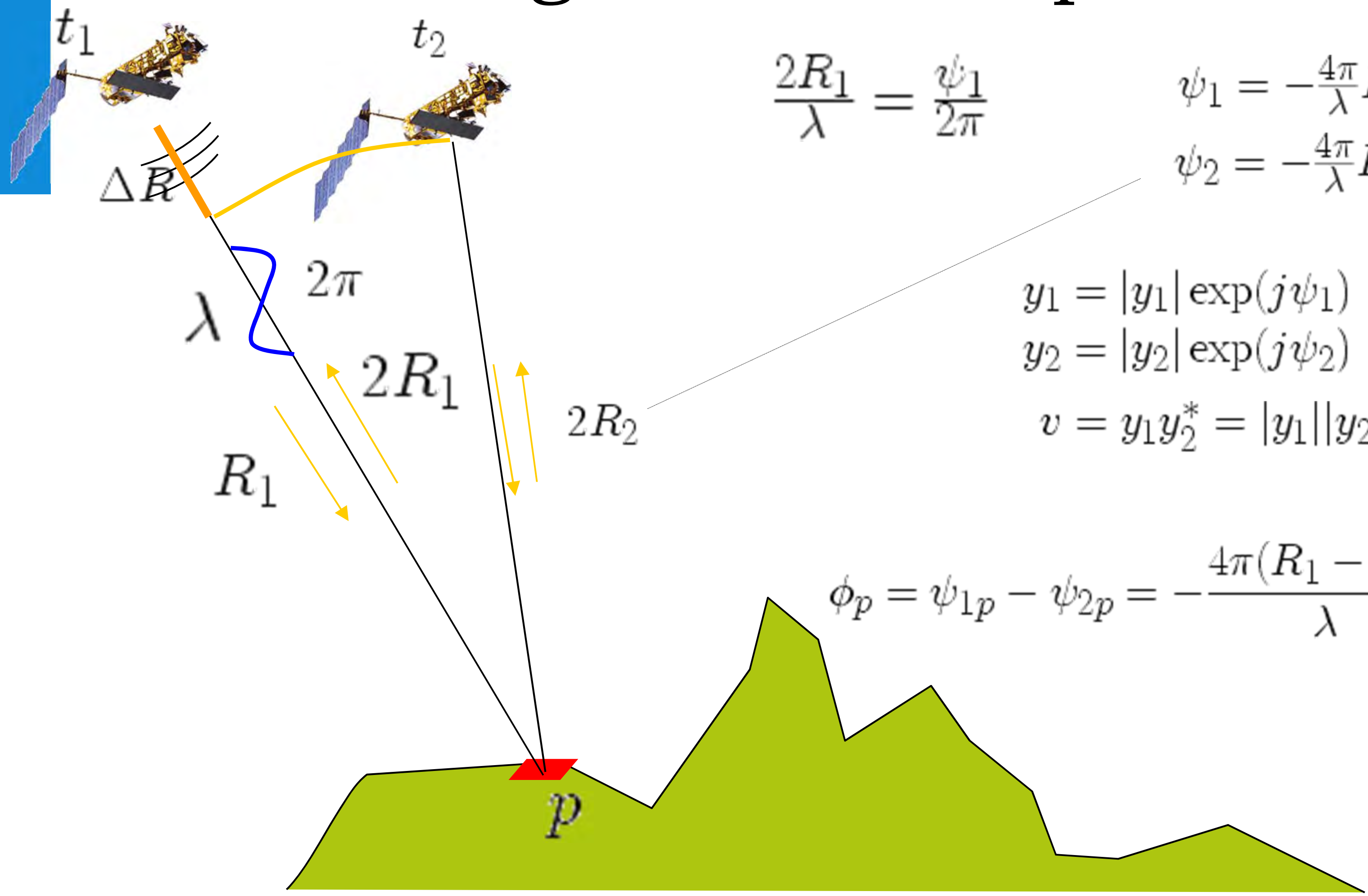

$$\frac{2R_1}{\lambda} = \frac{\psi_1}{2\pi}$$

$$\psi_1 = -\frac{4\pi}{\lambda}R_1$$
$$\psi_2 = -\frac{4\pi}{\lambda}R_2$$

$$y_1 = |y_1|\exp(j\psi_1)$$
$$y_2 = |y_2|\exp(j\psi_2)$$
$$v = y_1 y_2^* = |y_1||y_2|\exp(j(\psi_1 - \psi_2))$$

$$\phi_p = \psi_{1p} - \psi_{2p} = -\frac{4\pi(R_1 - R_2)}{\lambda} = -\frac{4\pi\Delta R}{\lambda}$$

This equation holds for dual-pass InSAR

Phase-height relationship

(Far-field approximation)

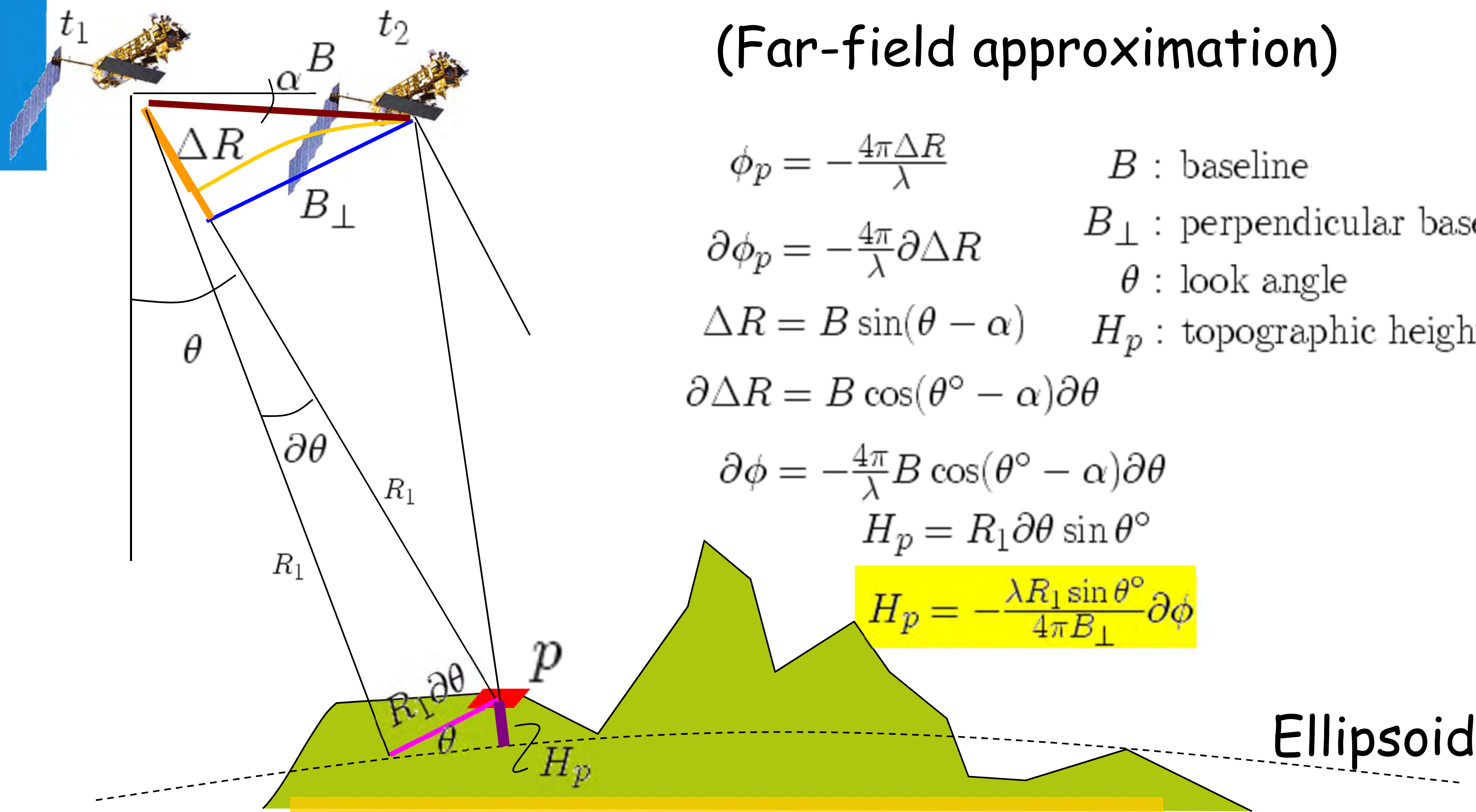

$$\phi_p = -\frac{4\pi\Delta R}{\lambda}$$

$$\partial\phi_p = -\frac{4\pi}{\lambda}\partial\Delta R$$

$$\Delta R = B\sin(\theta - \alpha)$$

$$\partial\Delta R = B\cos(\theta^\circ - \alpha)\partial\theta$$

$$\partial\phi = -\frac{4\pi}{\lambda}B\cos(\theta^\circ - \alpha)\partial\theta$$

$$H_p = R_1\partial\theta\sin\theta^\circ$$

$$H_p = -\frac{\lambda R_1\sin\theta^\circ}{4\pi B_\perp}\partial\phi$$

B : baseline

$B_\perp$: perpendicular baseline

θ : look angle

H_p : topographic height

Topographic phase is (inversely) scaled by the perpendicular baseline!

TU Delft

Topographic Phase

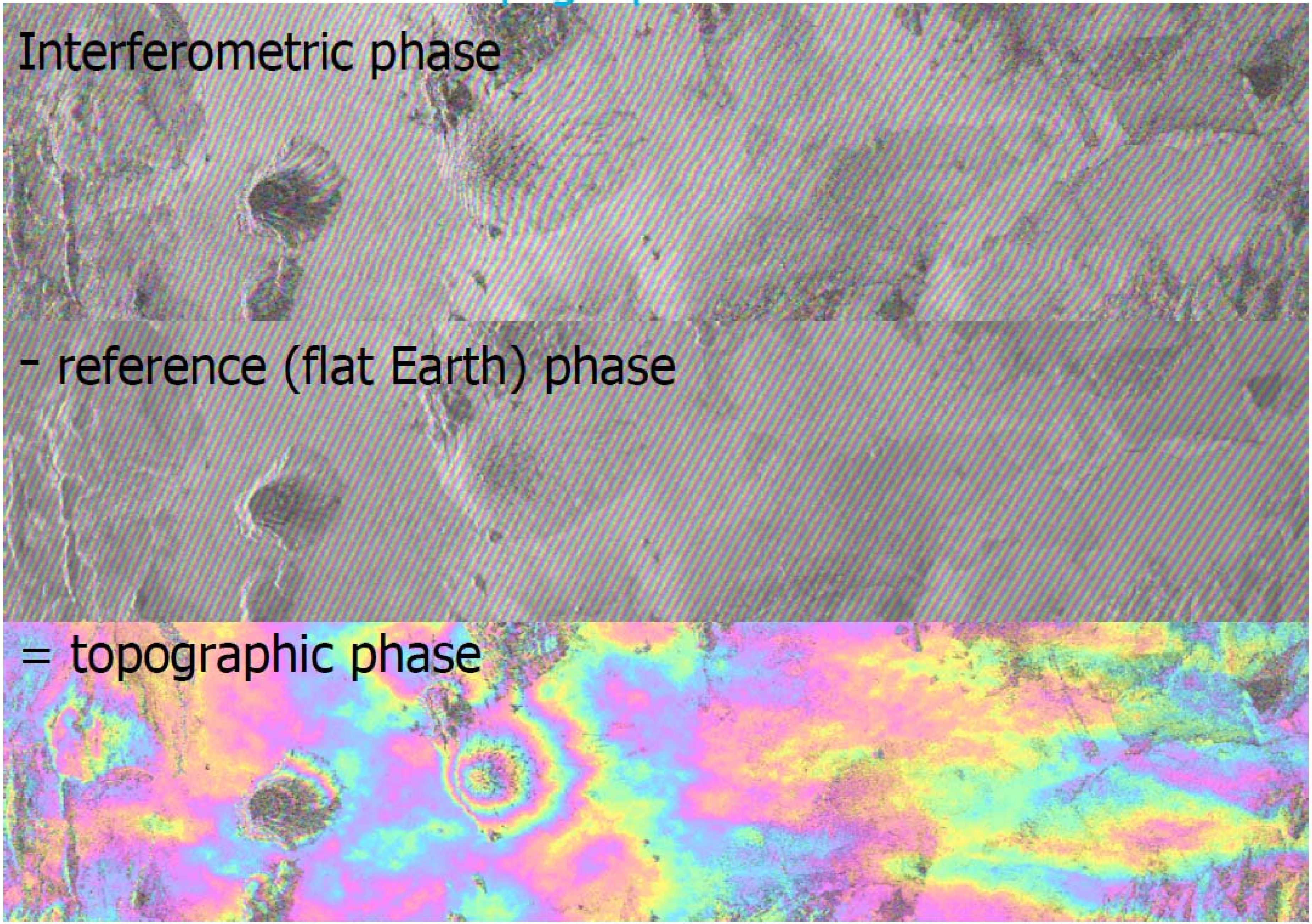

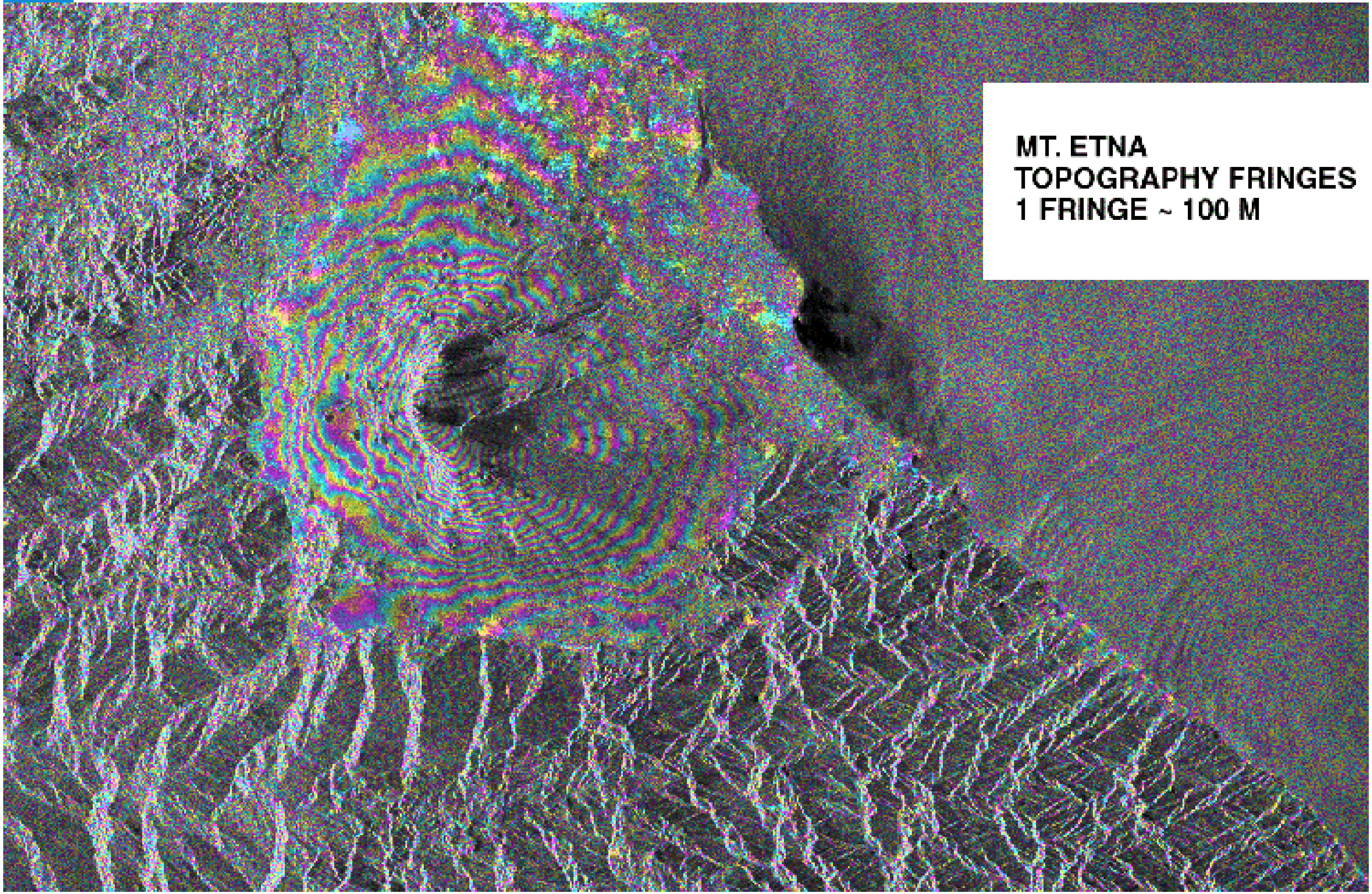
MT. ETNA
TOPOGRAPHY FRINGES
1 FRINGE ~ 100 M

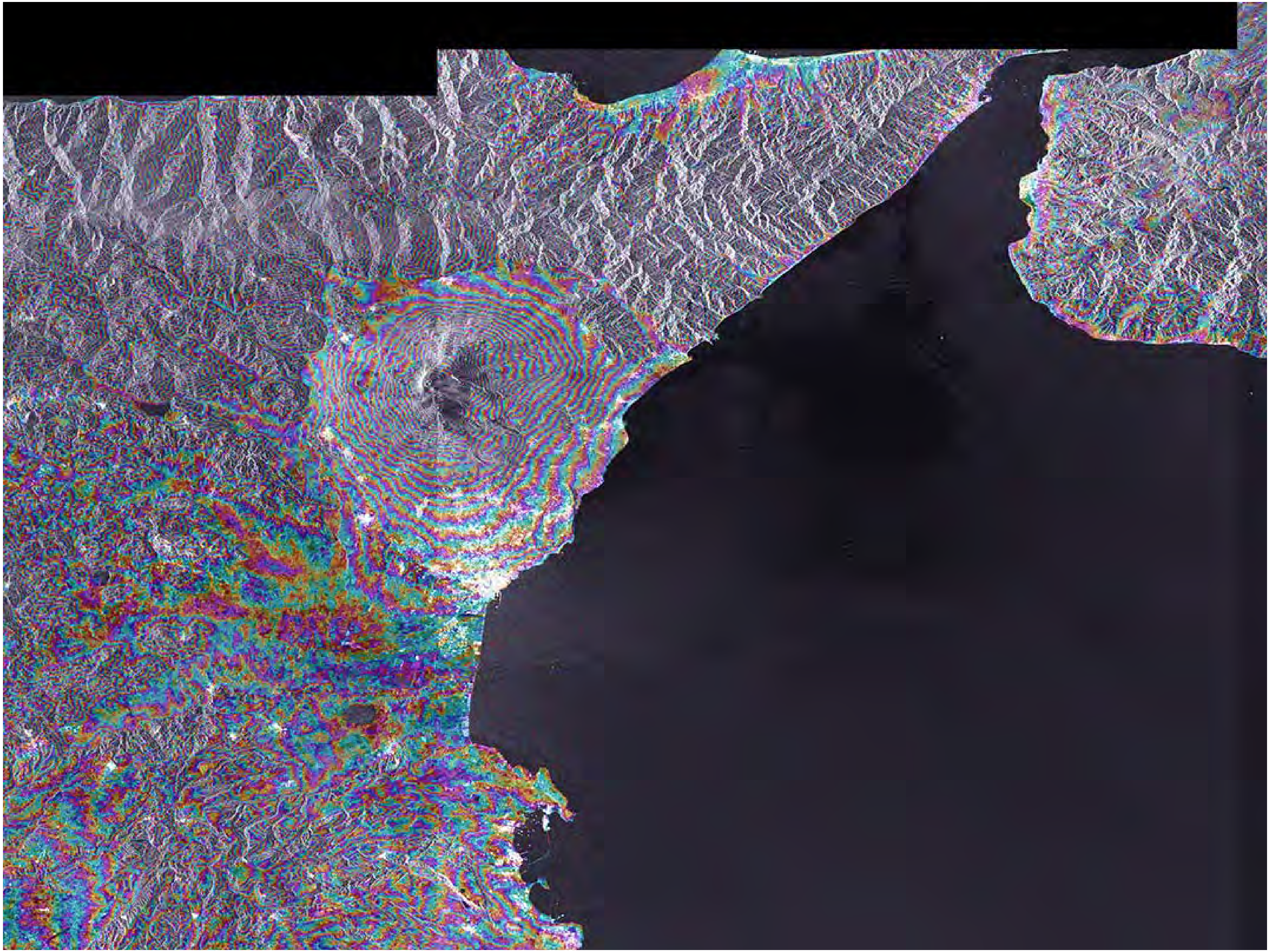

Height ambiguity

$$H_p = -\frac{\lambda R_1 \sin\theta^{\circ}}{4\pi B_{\perp}} \partial\phi$$

Height difference related to 1 phase cycle:

$$H_{2\pi} = \frac{-\lambda R_1 \sin\theta^{\circ}}{4\pi B_{\perp}} 2\pi = \frac{-\lambda R_1 \sin\theta^{\circ}}{2B_{\perp}}$$

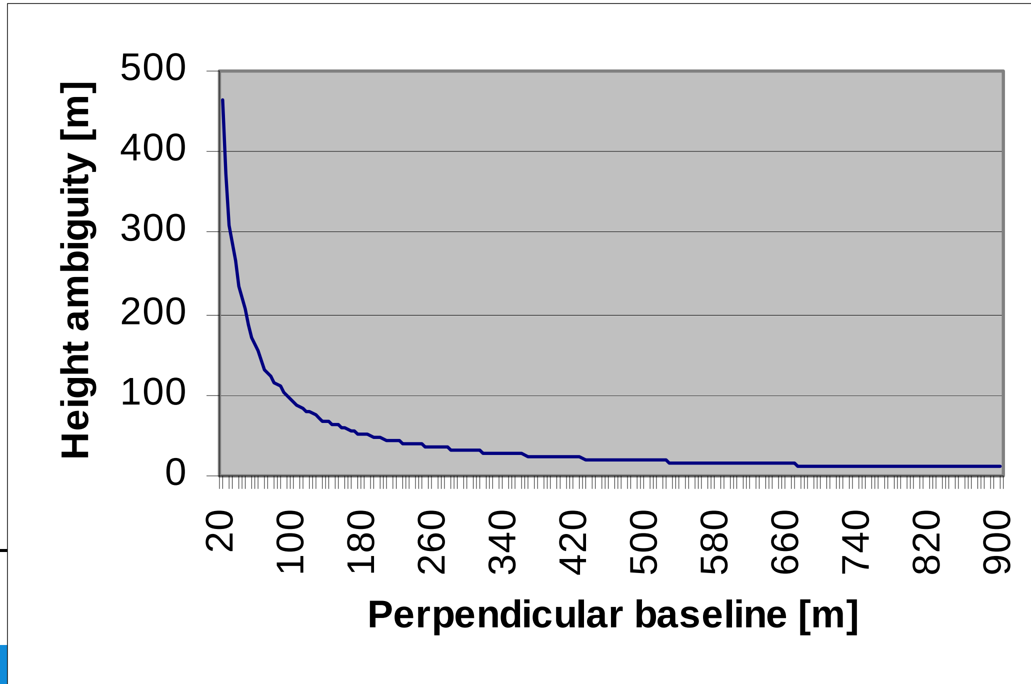

Baseline dependency, height ambiguity

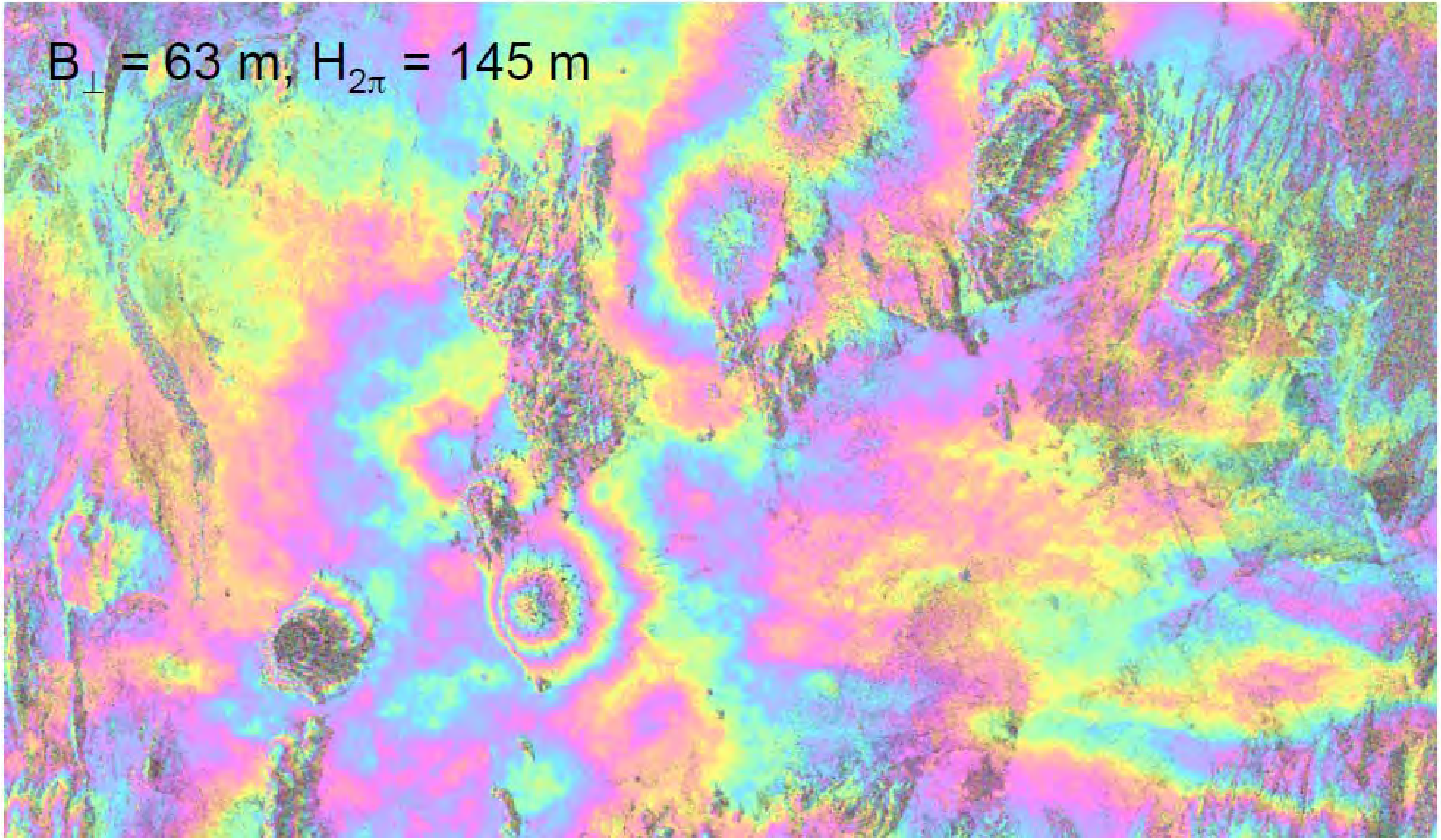

Baseline dependency, height ambiguity

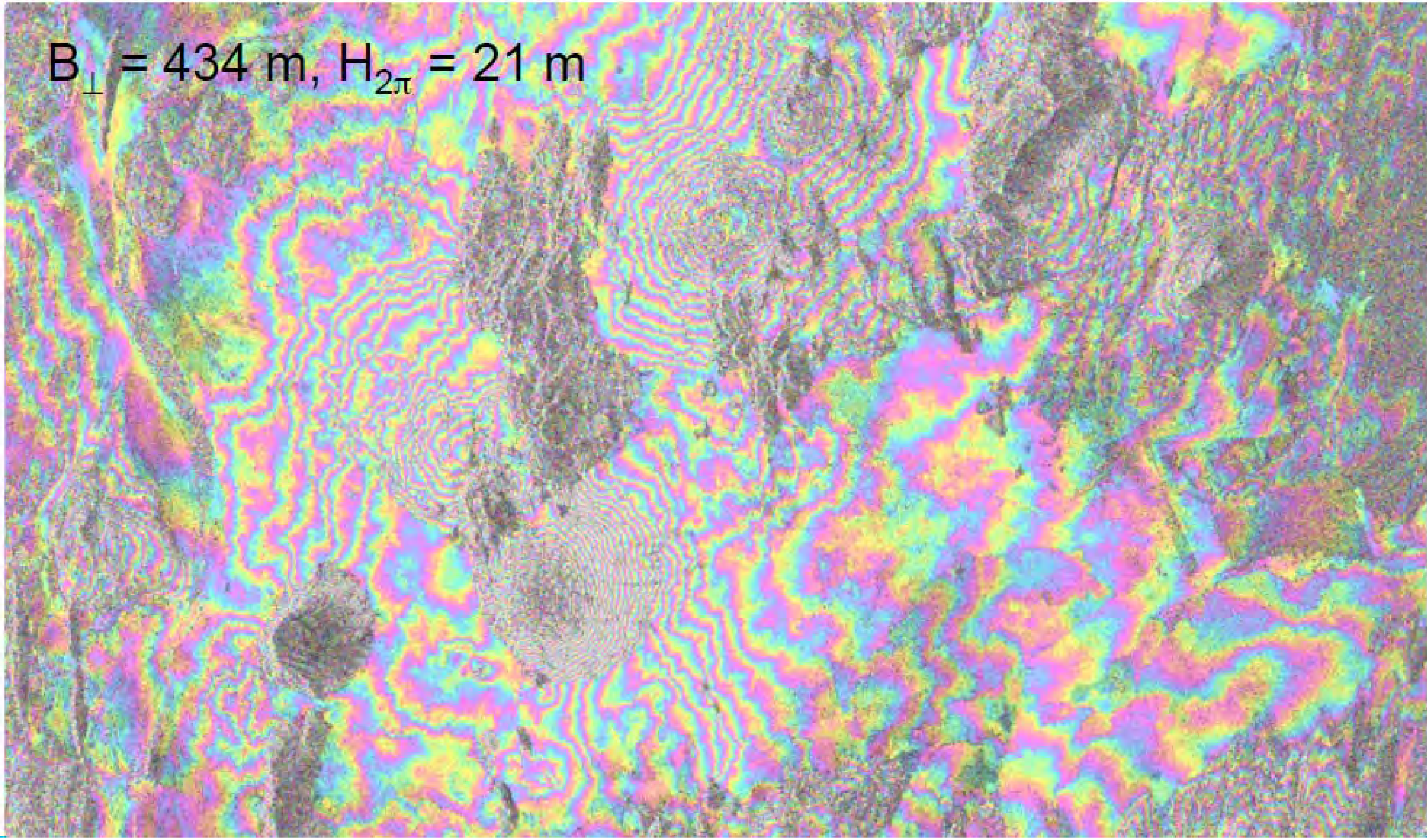

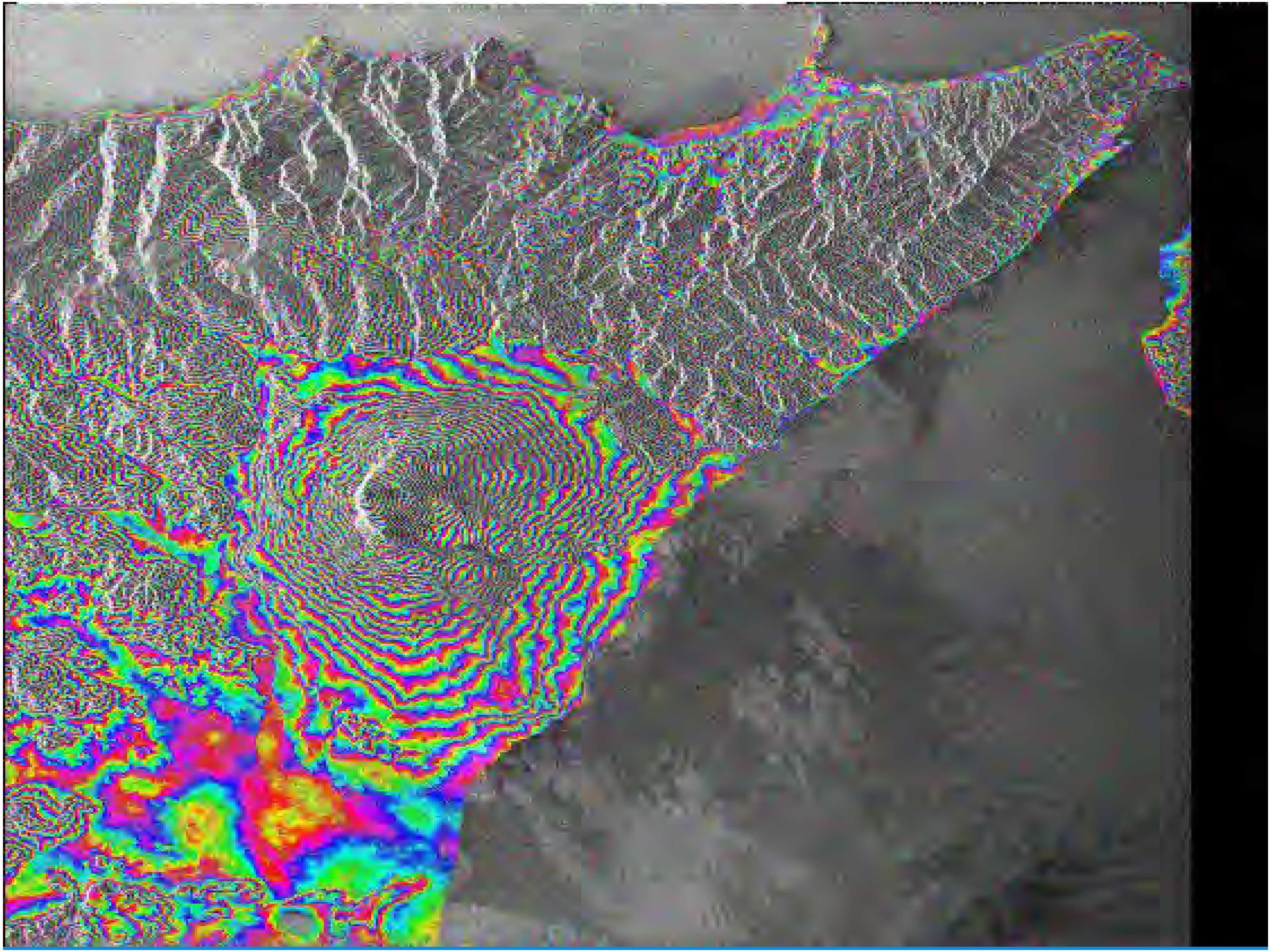

Baseline dependency, height ambiguity

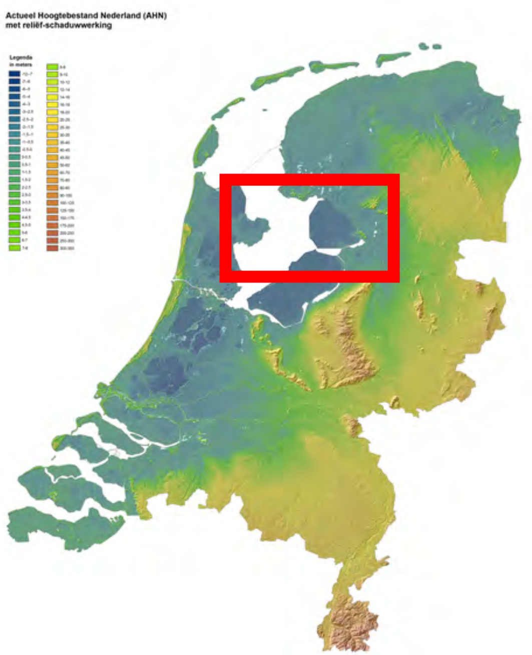

Bperp 173 m, Bt= 1day

H_{2pi}=45m

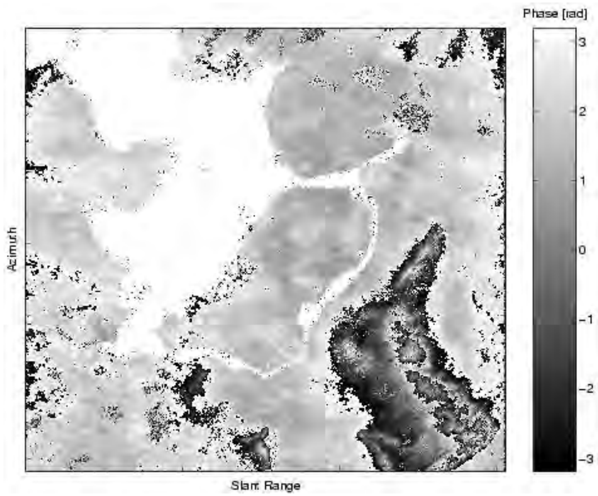

Bperp 531 m, Bt= 1 day

H_{2pi}=16m

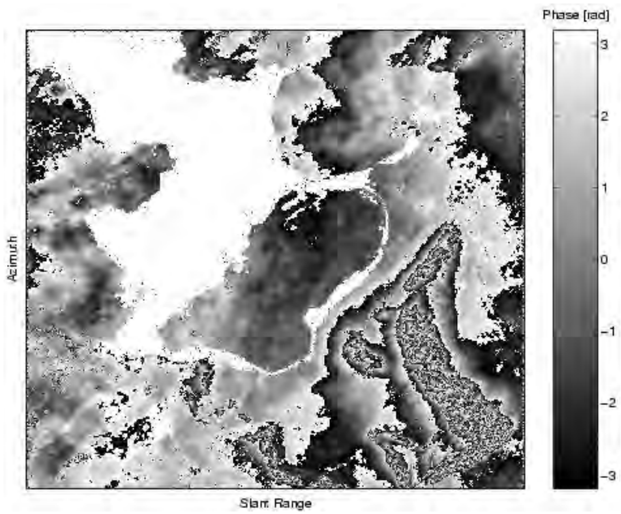

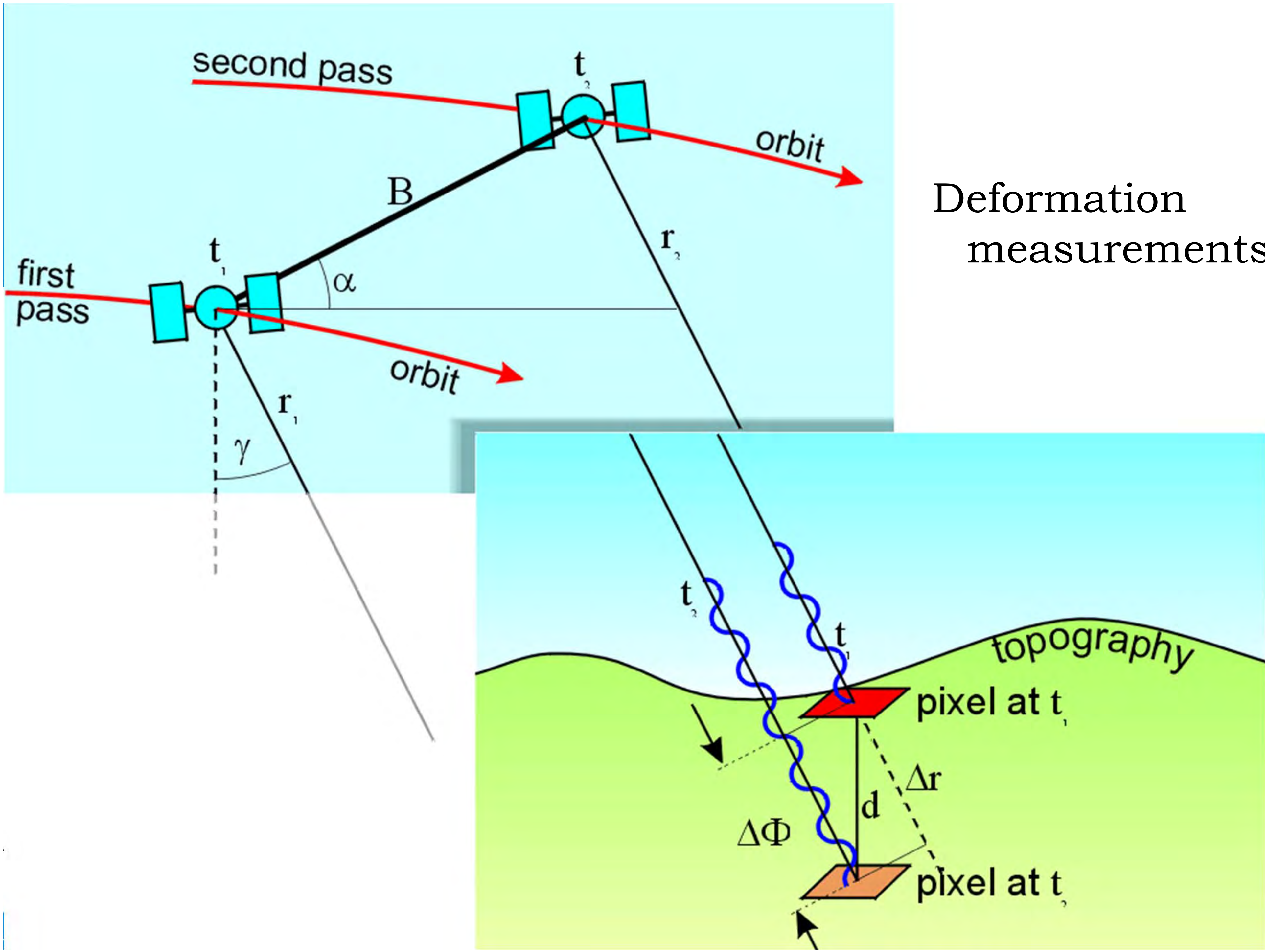

Deformation measurements

- Coseismic interferogram, showing deformation Izmit earthquake
- Every color cycle 7.5 cm horizontal motion
- Showing which segment of fault ruptured

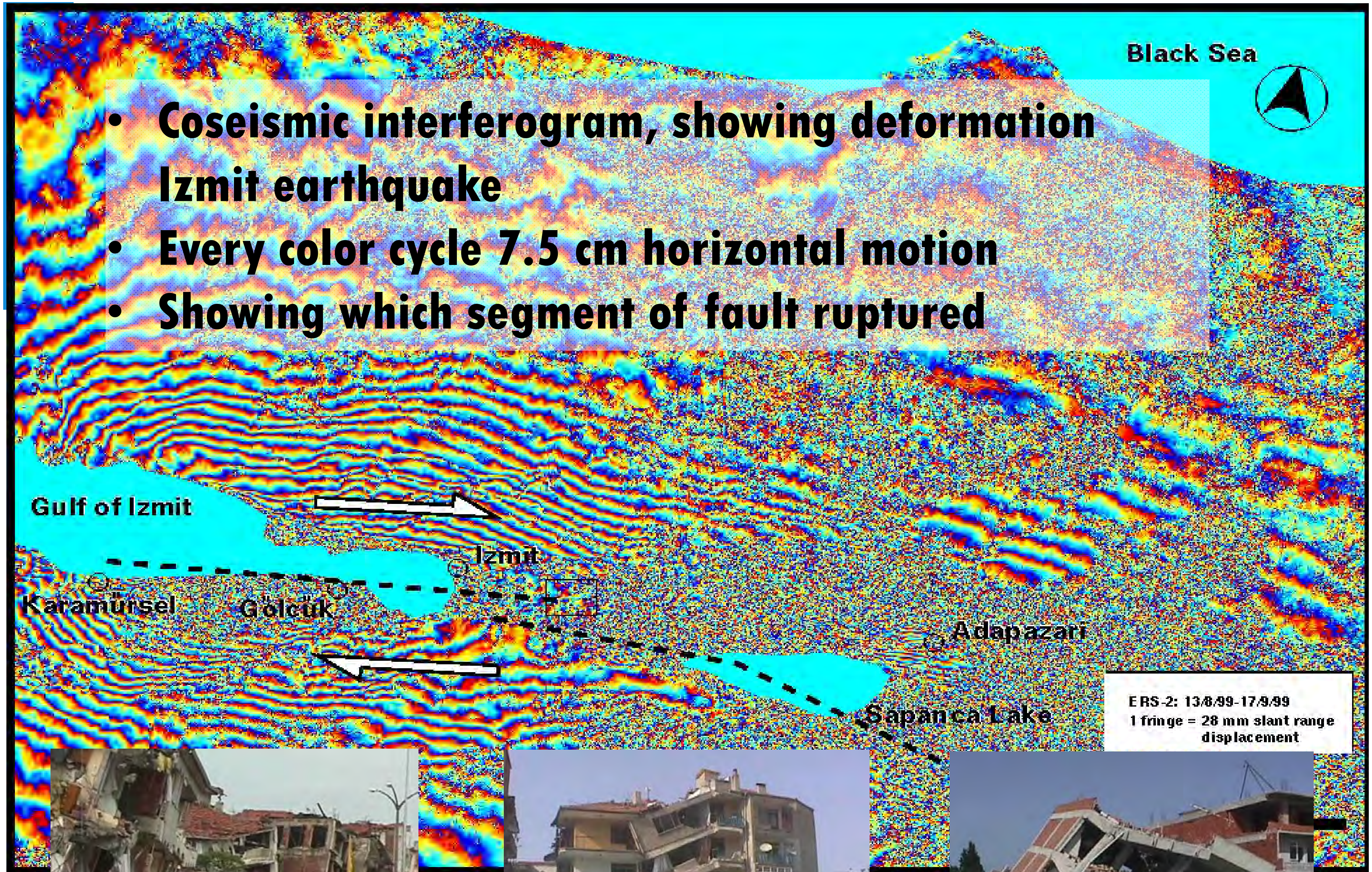

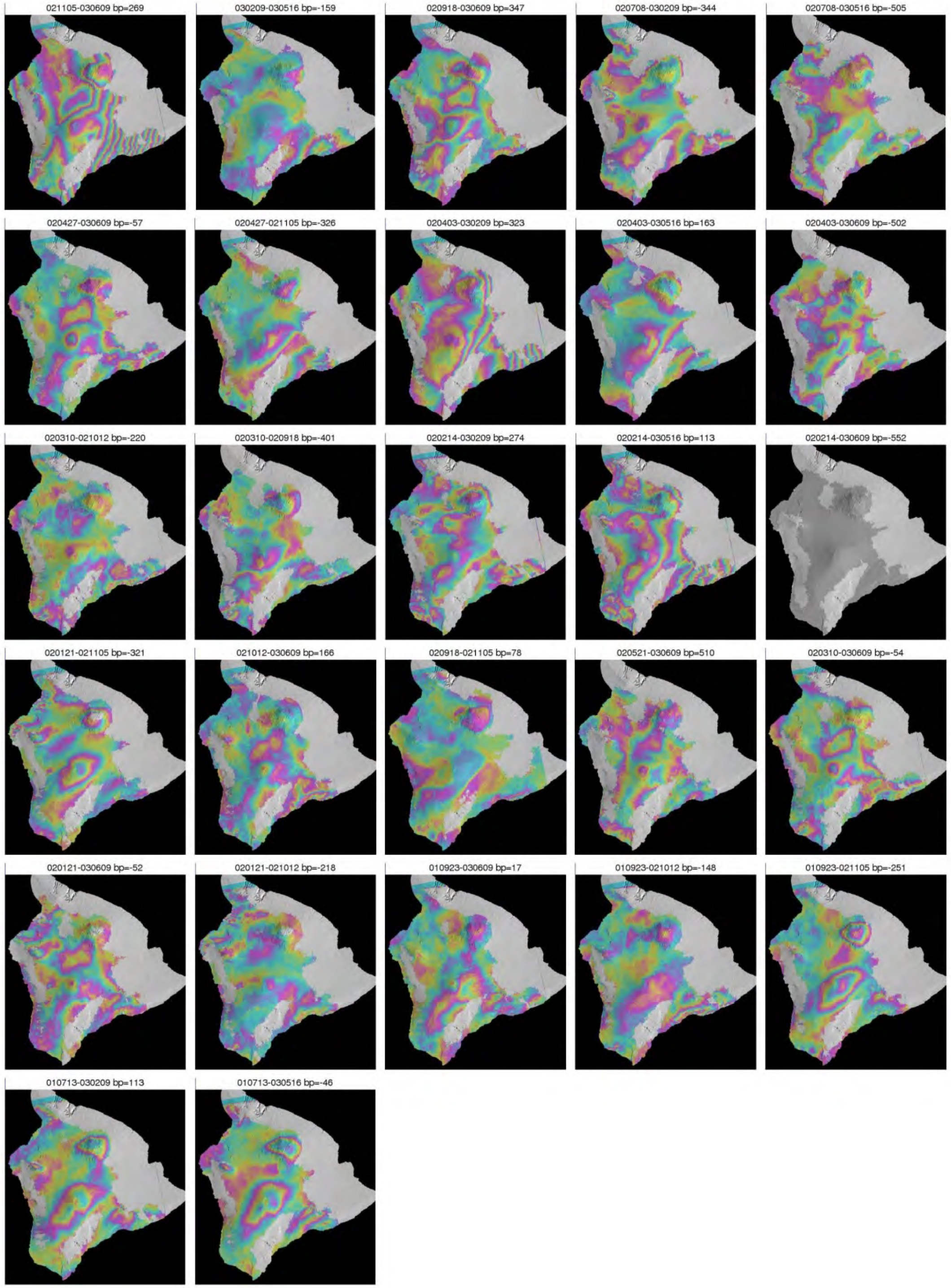

Mauna Loa, Hawaii

- Deformation (inflation) of the Mauna Loa summit
- Position of the magma chamber better determined

…Very sensitive to deformation

Subsidence Las Vegas due to ground water extraction

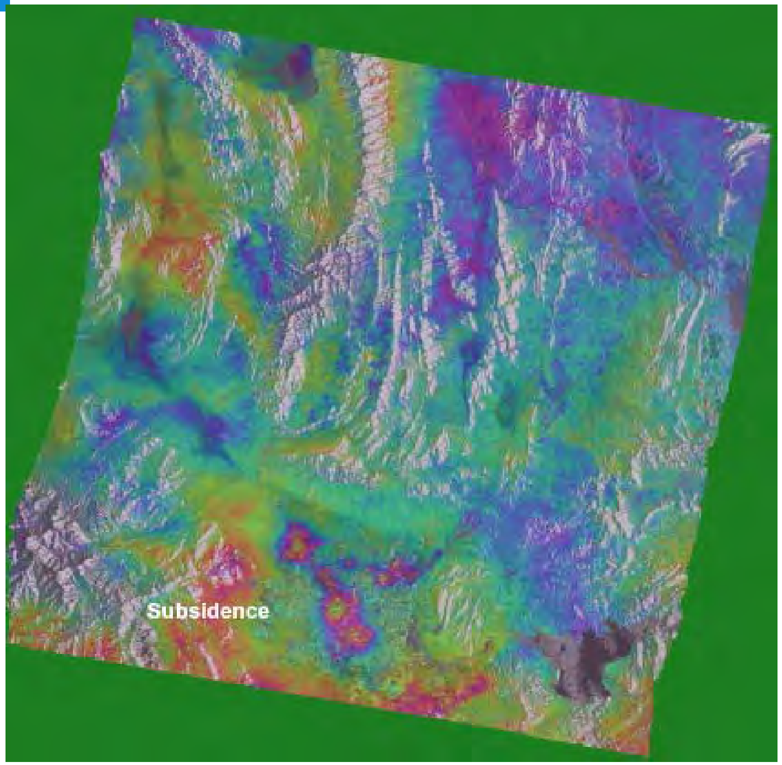

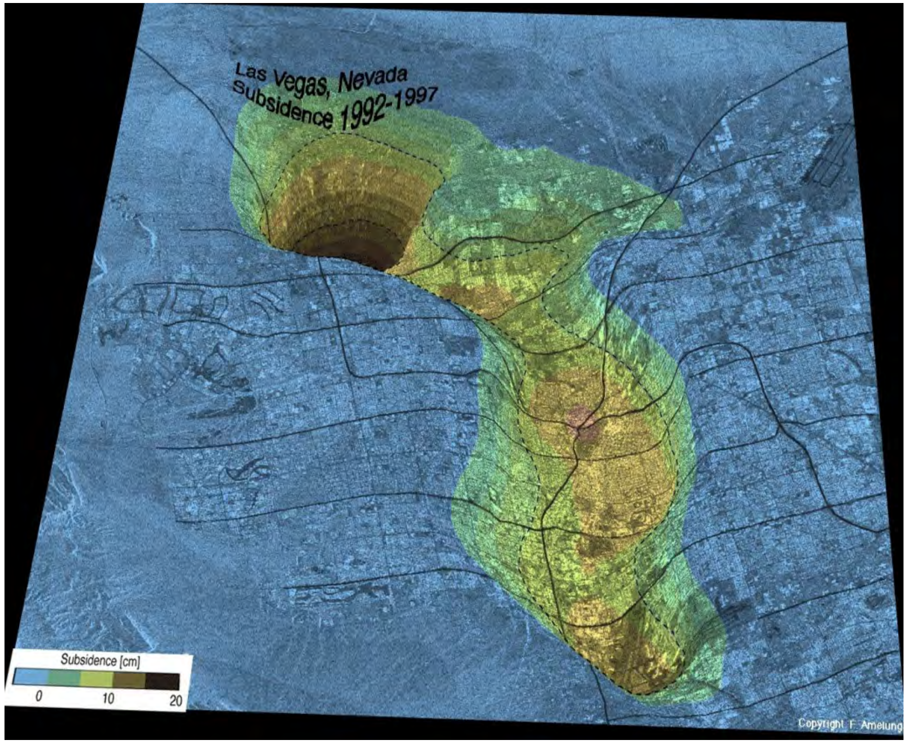

Image: Falk Amelung

Phase-deformation relationship

$$\frac{2R_1}{\lambda} = \frac{\psi_1}{2\pi}$$

$$\psi_1 = -\frac{4\pi}{\lambda}R_1$$
$$\psi_2 = -\frac{4\pi}{\lambda}R_2$$
$$R_2 = R_1 + D_p$$

$$\phi_p = \psi_{1p} - \psi_{2p} = -\frac{4\pi(R_1 - R_2)}{\lambda} =$$

$$\phi_p = -\frac{4\pi}{\lambda}D_p$$

D_p : line-of-sight deformation

1 cycle LOS deformation is equal to **half** the physical wavelength

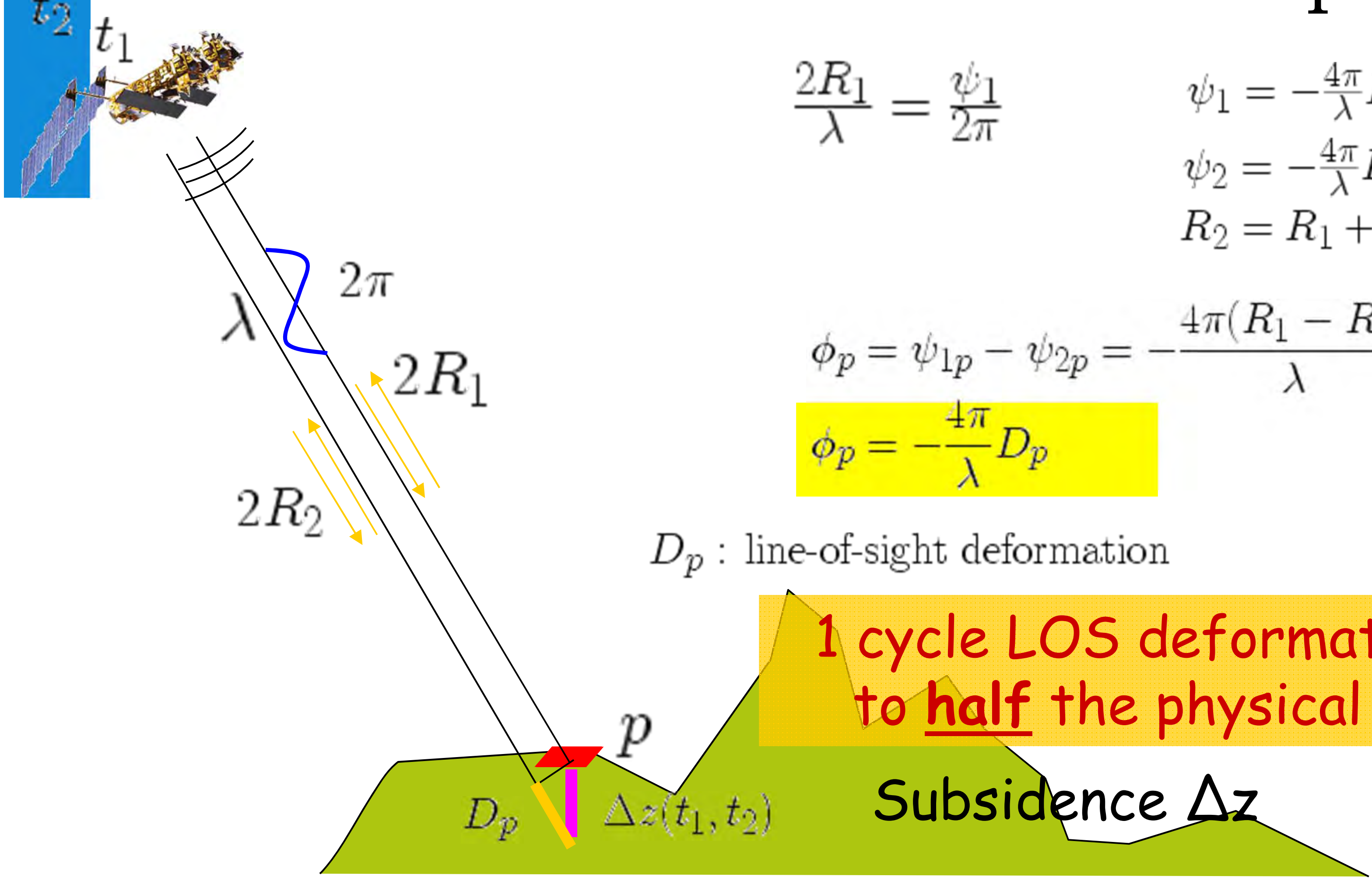

Topography and deformation

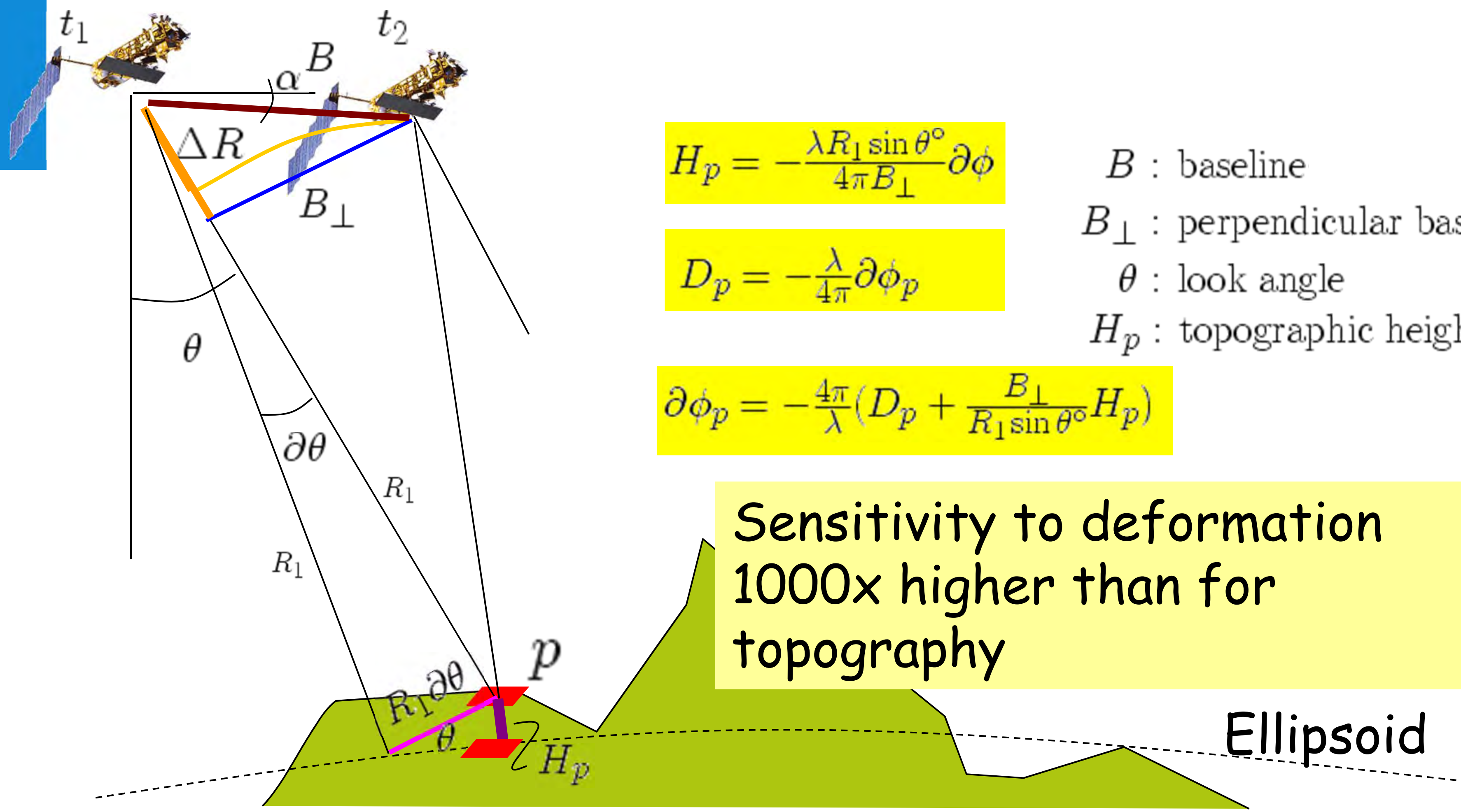

$$H_p = -\frac{\lambda R_1 \sin\theta^\circ}{4\pi B_\perp}\partial\phi$$

$$D_p = -\frac{\lambda}{4\pi}\partial\phi_p$$

$$\partial\phi_p = -\frac{4\pi}{\lambda}\left(D_p + \frac{B_\perp}{R_1 \sin\theta^\circ}H_p\right)$$

B : baseline
$B_\perp$: perpendicular baseline
θ : look angle
H_p : topographic height

Sensitivity to deformation 1000x higher than for topography

2ND LECTURE